ISSN 0105-8517

REGIONS OF ABSOLUTE STABILITY

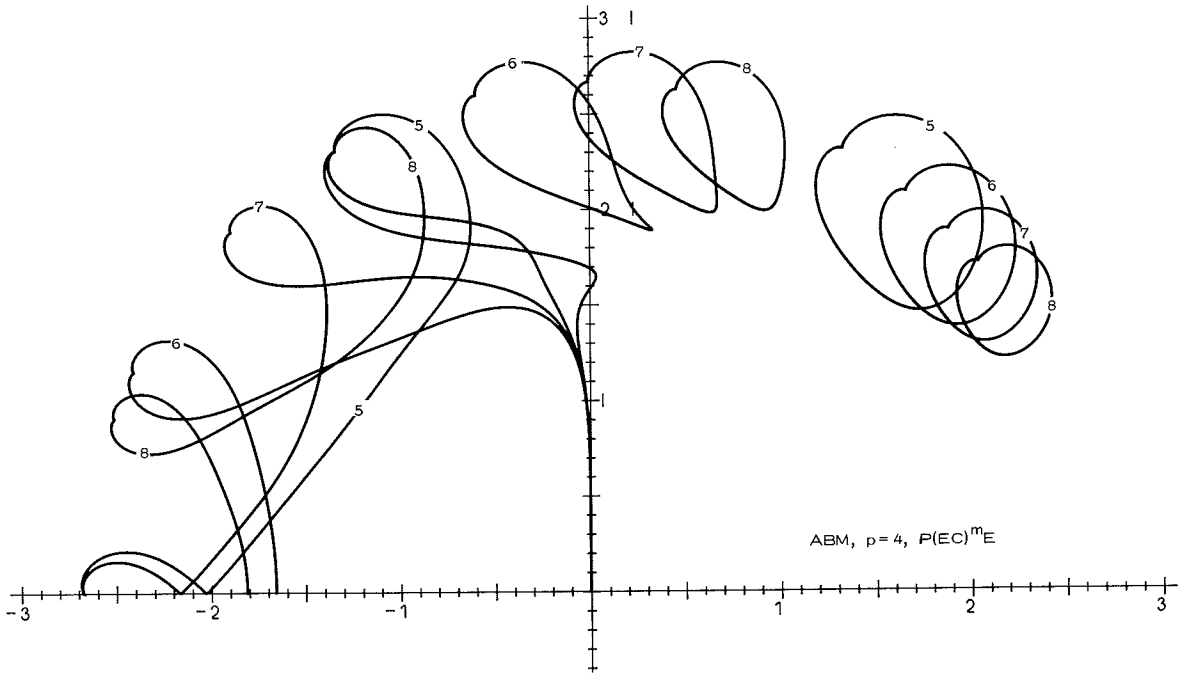

by
Jørgen Sand
Ole Østerby

DAIMI PB-102
September 1979

Computer Science Department
AARHUS UNIVERSITY
Ny Munkegade – DK 8000 Aarhus C – DENMARK
Telephone: 06 – 12 83 55

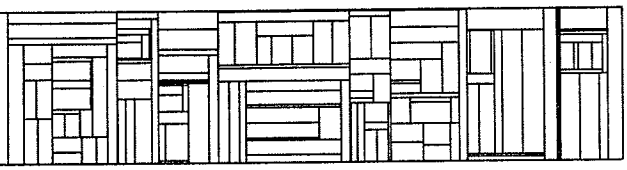

Abstract

At the Department of Computer Science a system has been developed for plotting regions of absolute stability for a large class of formulae and methods for solving systems of ordinary differential equations. This report is a pictorial guide through the stability regions of a number of well-known formulae thereby showing the capabilities of our programs, and hopefully also giving some new information about the methods.
In an appendix we give coefficients for Adams, Nyström, generalized Milne-Simpson and backward differentiation formulae up to order 12 (resp. 11) and coefficients for Padé approximations to the exponential up to degree 6.

Contents

1. Introduction

The study of stability properties of methods for the numerical solution of initial value problems goes back to the early 1950's with works of Dahlquist [6] and Rutishauser [22]. In 1956 [7] Dahlquist proved the fundamental theorem for linear multistep methods which in modern formulation can be phrased :

$$\text{consistency} + \text{stability} \Longleftrightarrow \text{convergence},$$

and he also introduced the first Dahlquist-barrier : The order of a stable linear k-step method cannot exceed $k+2$.

The above-mentioned convergence is with respect to the limit, $h \to 0$, and the significance is that when using a convergent method it is in theory possible to get arbitrarily accurate solutions by reducing the step-size, h. But in practice we are not interested in using extremely small step-sizes and accuracy is also destroyed by unavoidable round-off errors. And for calculations with finite h the above-mentioned stability is not enough to ensure reasonable results. The use of electronic computers with their capacities for very long sequences of unsupervised calculations also pressed the need for new stability concepts and for a disciplined use of the word stability.

In the following we shall use the terminology of Lambert [15] who uses the name 0-stability for the concept which Dahlquist introduced. Among the various stability concepts which saw the light of day we have focused our attention mainly on the absolute stability (see next section) but some of our investigations are useful also for the study of exponential stability (see section 13).

With specific reference to the so-called stiff problems Dahlquist introduced A-stability [8] and also erected the second Dahlquist barrier : The order of an A-stable linear multistep method cannot exceed 2.

In attempts to avoid this barrier a new host of stability concepts was introduced such as $A(\alpha)$-stability [32] and stiff stability [11] to name two.

At present we have very good tools - including what is presented in this report - for studying these types of stability which can be grouped together with the term : linear stability theory. In years to come we shall see more work devoted to relative stability concepts and stability for non-linear systems.

2. Absolute Stability

We shall study the stability properties of certain methods for the solution of initial value problems

$$y' = f(x,y) \quad , \quad y(x_0) = y_0 \, .$$

The method is applied to the linear, homogeneous test equation

$$y' = \lambda y \quad , \quad y(0) = 1 \quad , \quad \lambda \in \acute{C}$$

with constant step size h, thus producing a linear difference equation. The characteristic polynomial of this difference equation is also called the stability polynomial.

A method is called absolutely stable for a particular value of $h\lambda = \bar{h}$ if all roots of the stability polynomial have modulus less than one. The set of all such real $\bar{h}$ is called the stability interval. The set of all such $\bar{h} \in \acute{C}$ is called the region of absolute stability. Inside (and on most of the boundary of) this region all solutions of the difference equation are bounded and this is a desirable feature if $Re(\bar{h}) \leq 0$ because then the solution of the differential equation is bounded.

Some authors also allow values of $\bar{h}$ that give rise to simple roots of modulus one. This corresponds completely to the boundedness criterion, but the difference is insignificant in practice as it only amounts to including (part of) the boundary into the stability region. But in this case a 0-stable method always has an absolute stability region, although possibly with an empty interior (example : a weakly stable method such as the midpoint rule).

If one has access to a digital computer with graph plotting equipment, a convenient way of determining the region of absolute stability is the so-called boundary locus method [15, p. 82], which amounts to tracing the curve(s) in the complex plane corresponding to the case that one root of the stability polynomial is of the form $\exp(i\theta)$. Thereby the complex plane is divided into one or more regions characterized by the number of roots which are greater than one. This number can, because of con-

tinuity, not vary within a connected region, but only when crossing the boundary locus curve. An additional calculation of all roots of the stability polynomial, carried out for one point inside each region, suffices to determine this number. The region of absolute stability is characterized by the number 0. It is not necessary to compute the roots as we are only interested in their magnitudes relative to one. Therefore, the Schur-type method due to Miller [17] can be used to advantage saving a good deal of arithmetic operations.

Actually only one test needs to be performed if one applies a counting argument due to Dahlquist [9, p. 80] and derived using the properties of conformal mappings. If we keep track of the direction of movement of the boundary locus curve as θ increases from 0 to 2π, then the number of roots larger than one to the left of the curve is always one smaller than the number to the right of the curve if the curve is traversed only once. Or (with kind thoughts to electromagnetism) if one places the right hand on the boundary locus curve with the fingers pointing in the direction of travel then the thumb points to the side where there is one root less of magnitude larger than one. We shall refer to this rule as : Dahlquist's right hand rule.

Dahlquist's result which he mentions in connection with linear multistep methods applies also to predictor-corrector methods and a straightforward generalization is possible for curves that are traversed more than once (e. g. the midpoint rule, and Milne's predictor).

At the Computer Science Department at Aarhus University a system has been developed to draw regions of absolute stability as outlined above. A further description of the system and a user manual is found in [24].

In this report we shall show examples of the performance of the system but with emphasis on drawing stability regions for well-known formulae for the sake of comparing the various formulae in various modes and of various orders.

3. Linear Multistep Formulae

A linear multistep formula is written in the form

$$(1) \quad \sum_{j=0}^{k} \alpha_j y_{n+j} = h \sum_{j=0}^{k} \beta_j f_{n+j} \quad , \quad \alpha_k = 1 .$$

We define the first and the second stability polynomials by

$$\rho(z) = \sum_{j=0}^{k} \alpha_j z^j \quad ; \quad \sigma(z) = \sum_{j=0}^{k} \beta_j z^j .$$

The stability polynomial of formula (1) is then

$$(2) \quad \pi(z, \bar{h}) = \rho(z) - \bar{h}\, \sigma(z) ,$$

and the boundary locus curve is found by setting

$$\bar{h} = \frac{\rho(z)}{\sigma(z)} \quad , \quad z = e^{i\theta} \quad , \quad 0 \le \theta \le 2\pi .$$

The boundary locus curve (and the stability region) is symmetric about the real axis and we can find the part which lies in the first and second quadrant by letting $0 \le \theta \le \pi$ and reflecting possible parts that lie below the real axis. We shall in most cases only draw this part of the curve.

Fig. 1 shows the complete boundary locus curve $(0, 2\pi)$ for the fifth order explicit Nyström formula. We have indicated the direction of motion as θ increases as well as the number of roots larger than one in magnitude such that the figure serves as an illustration of the right hand rule. We note that there is no absolute stability region for this formula. Fig. 2 shows in a similar manner the boundary locus curve for the 6th order Adams-Bashforth formula. We have cut away the large loops, which extend to $+14$, in order to show the details around the origin.

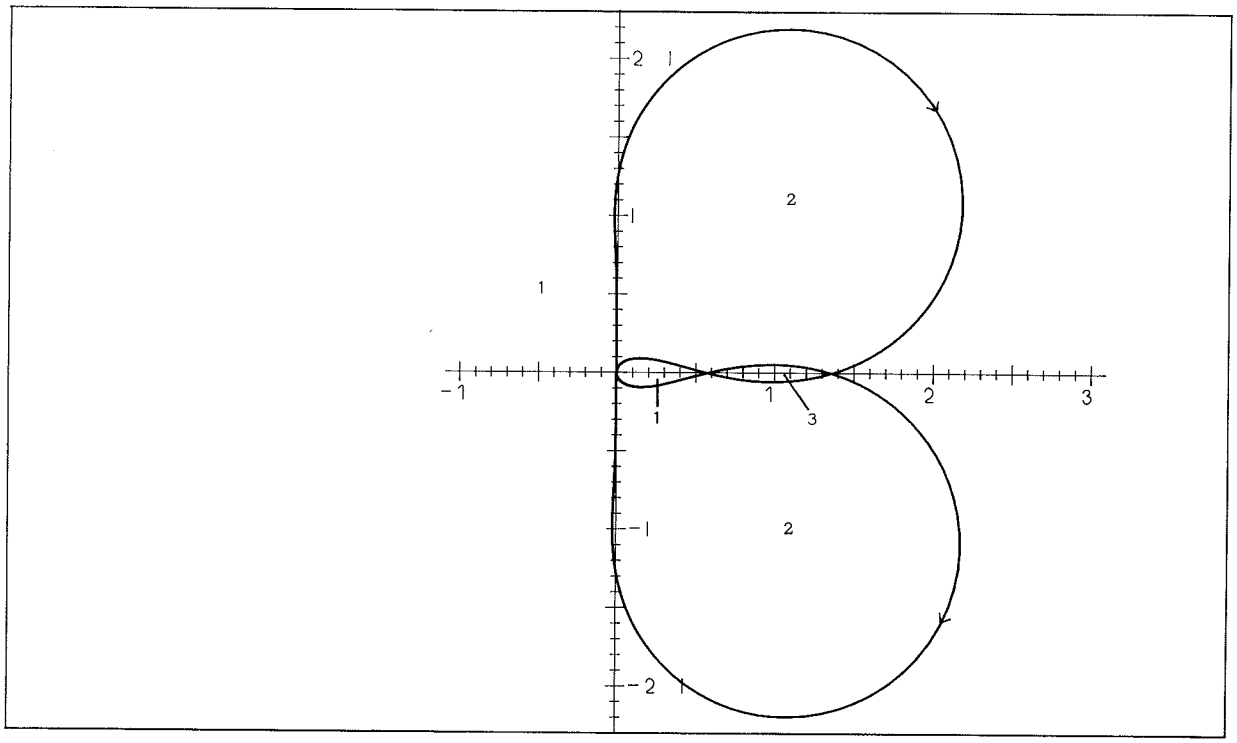

Fig. 1. Nyström predictor of order 5.

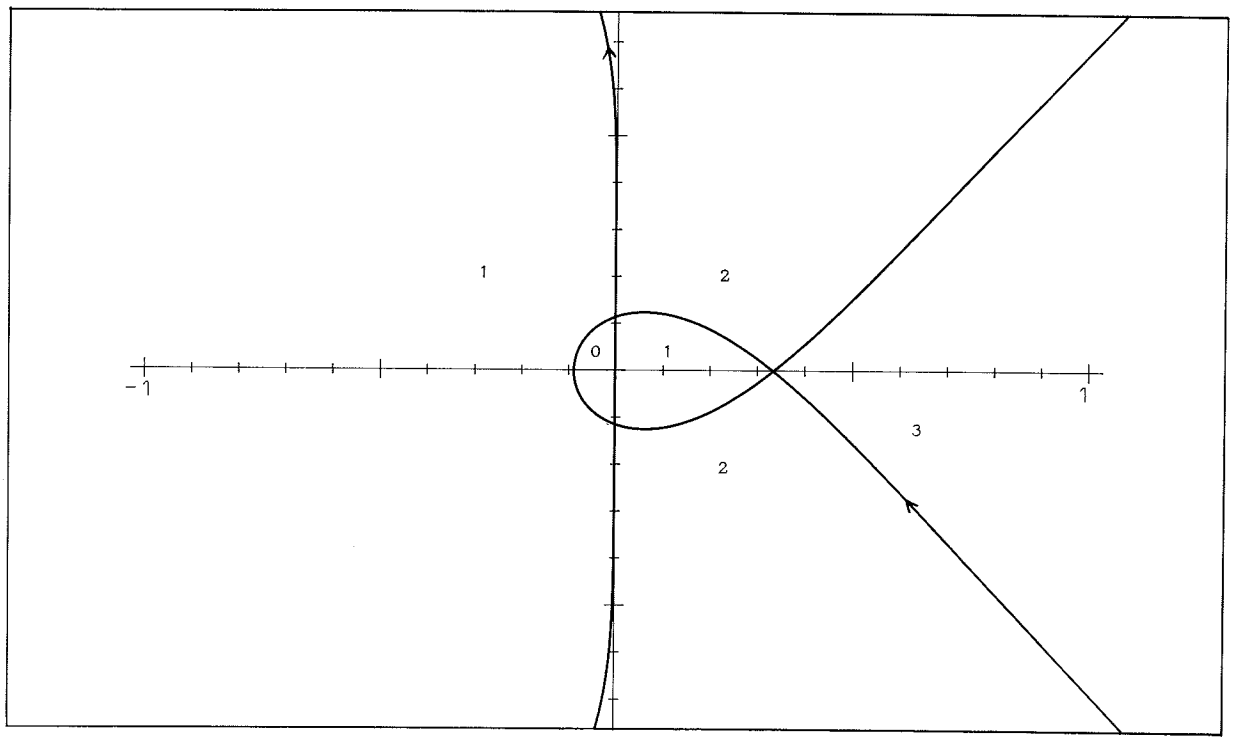

Fig. 2. Adams-Bashforth predictor of order 6.

Boundary locus curves. The numbers indicate number of roots larger than 1 in each region.

In fig. 3 we have collected the boundary locus curves for the Adams-Bashforth explicit formulae of orders 2 to 6 and in fig. 4 we show those of the Nyström formulae of the same orders. Fig. 5 and 6 show the boundary locus curves for the Adams-Moulton implicit formulae of orders 2 to 6 and the generalized Milne-Simpson implicit formulae of orders 4 to 7 respectively. Only part of the curve for the second order Adams-Moulton formula (the trapezoidal rule) is drawn; it is the imaginary axis. All the Adams formulae have an absolute stability region (immediately to the left of the origin) which decreases with the order. None of the Nyström and Milne-Simpson formulae have a stability region according to our definition, which excludes roots of modulus equal to one.

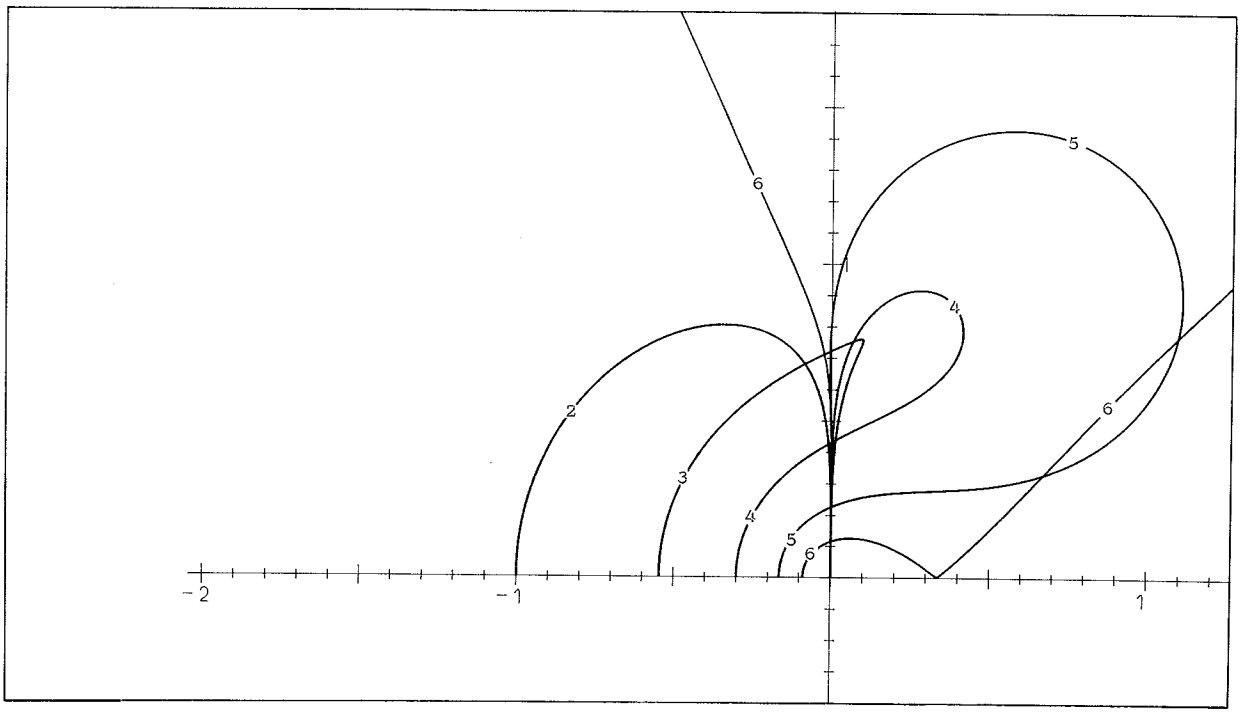

Fig. 3. Adams-Bashforth predictors, orders 2-6.

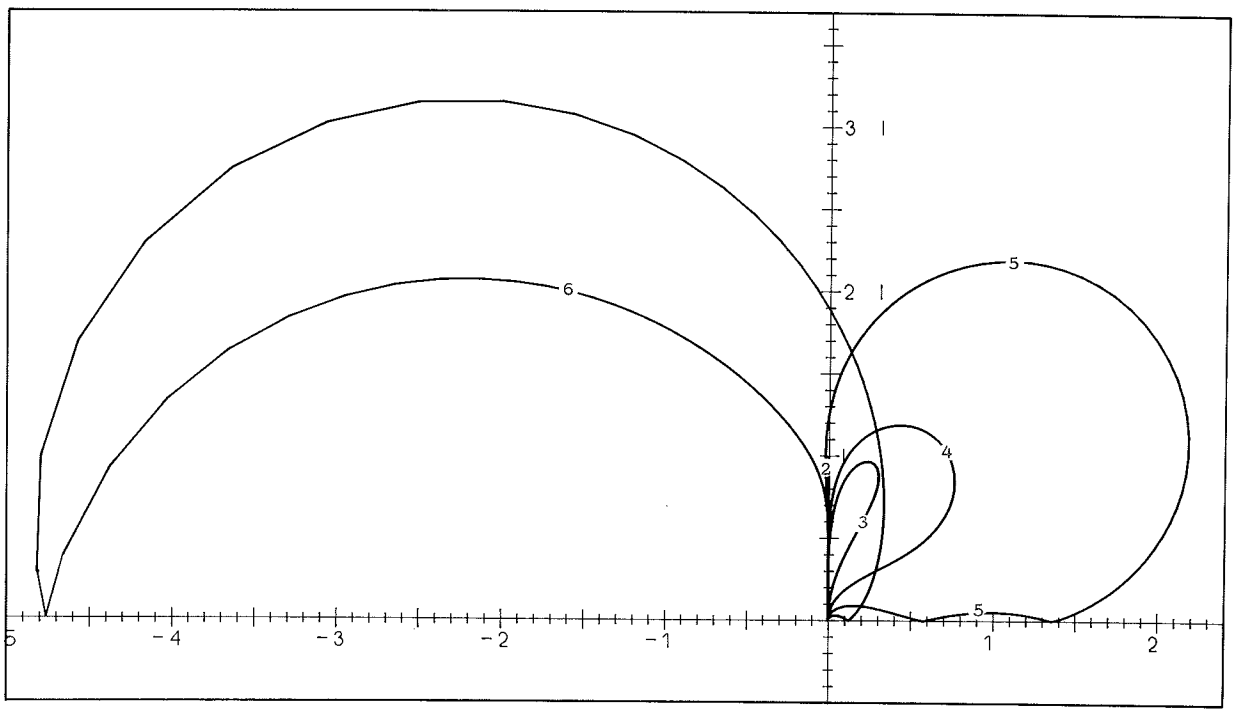

Fig. 4. Nyström predictors, orders 2-6.

Boundary locus curves. The numbers indicate the order of the method.

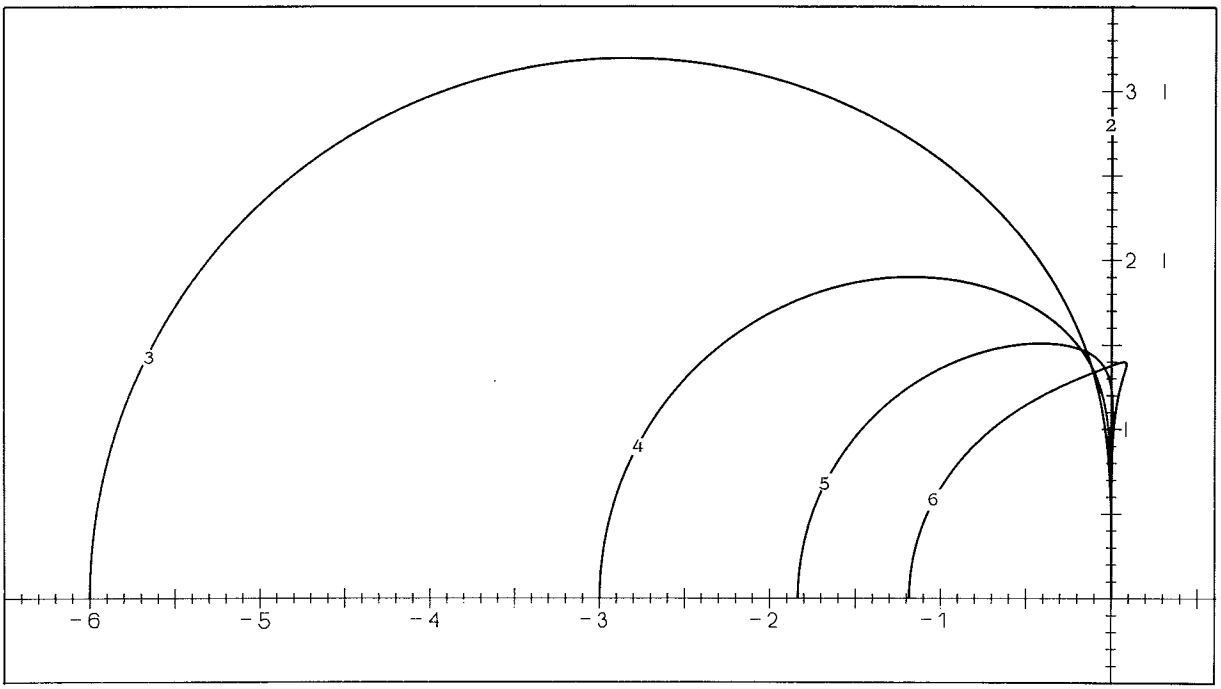

Fig. 5. Adams-Moulton correctors, orders 2-6.

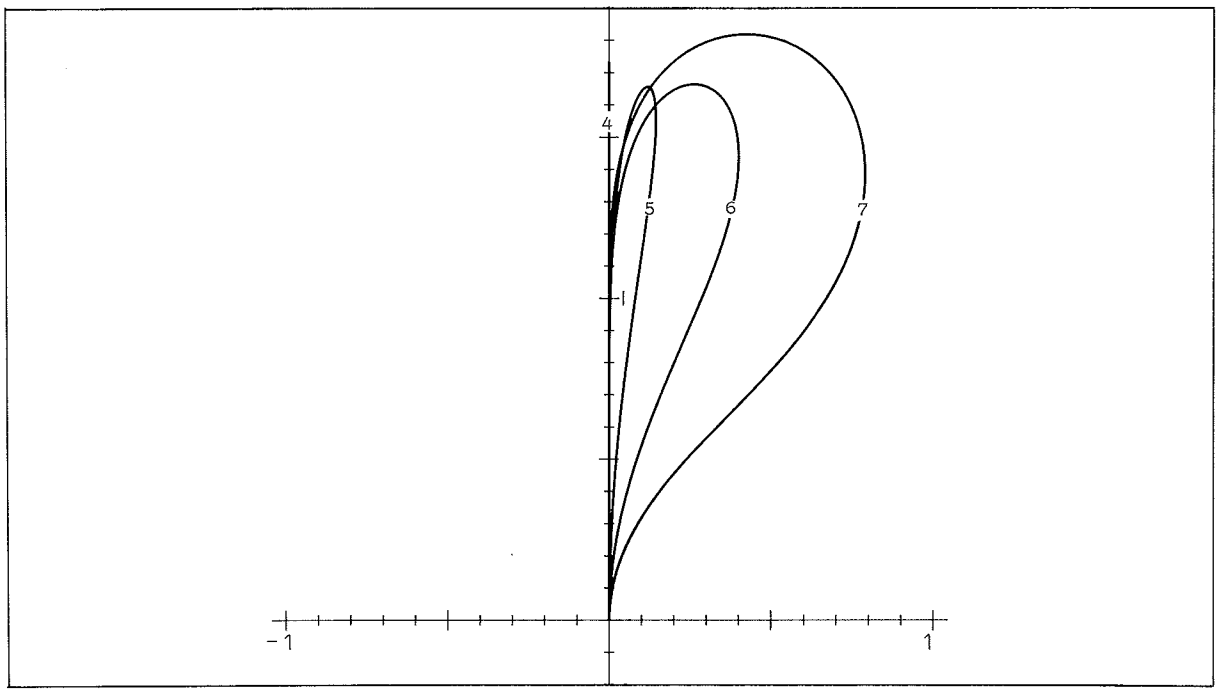

Fig. 6. Generalized Milne-Simpson correctors, orders 4-7.

Boundary locus curves. The numbers indicate the order of the method.

4. Predictor-Corrector Methods

When an explicit and an implicit linear multistep formula are used together as a predictor-corrector pair the region of absolute stability will depend on the stability polynomials of both formulae and of the mode. If the first and second polynomials are denoted $\rho^*(z)$ and $\sigma^*(z)$ for the predictor and $\rho(z)$ and $\sigma(z)$ for the corrector (see (2)), then the stability polynomial for the predictor-corrector method in $P(EC)^mE$-mode ($m \geq 1$) is [15, p. 97]:

$$(3) \quad \pi(z,\bar{h}) = \rho(z) - \bar{h}\,\sigma(z) + M_m(\bar{h}) \cdot [\rho^*(z) - \bar{h}\,\sigma^*(z)]$$

where

$$(4) \quad M_m(\bar{h}) = (\bar{h}\,\beta_k)^m \, \frac{1 - \bar{h}\,\beta_k}{1 - (\bar{h}\,\beta_k)^m} \; .$$

For $P(EC)^m$ mode we have [15, p. 98]

$$(5) \quad \pi(z,\bar{h}) = \beta_k z^k [\rho(z) - \bar{h}\,\sigma(z)] + M_m(\bar{h}) \cdot [\rho^*(z)\,\sigma(z) - \rho(z)\,\sigma^*(z)] \; .$$

For $m > 1$, resp. 2 we cannot solve explicitly for $\bar{h}$. In order to determine the boundary locus curve we shall in general have to use a root-finding routine to determine $m + 1$, resp. m values of $\bar{h}$ for each value of θ. Thus the boundary locus curve will often consist of several curves as seen in fig. 7 for the classical Milne's method [18, p. 66], [15, p. 93] in PECE mode. The boundary locus curve for Milne's predictor is the imaginary axis traversed twice upwards, and there is one root of modulus larger than one in the left half-plane and three in the right half-plane. The boundary locus curve for Milne's corrector is the interval $[-i\sqrt{3},\ i\sqrt{3}]$ on the imaginary axis (traversed up and down again) and there is one root of modulus larger than one in each half-plane. Thus neither the predictor nor the corrector has a region of absolute stability. Nevertheless, Milne's method has a stability interval which is roughly $(-.85, -.30)$ and a stability region thereabout as seen on fig. 7. Unfortunately, 0 is

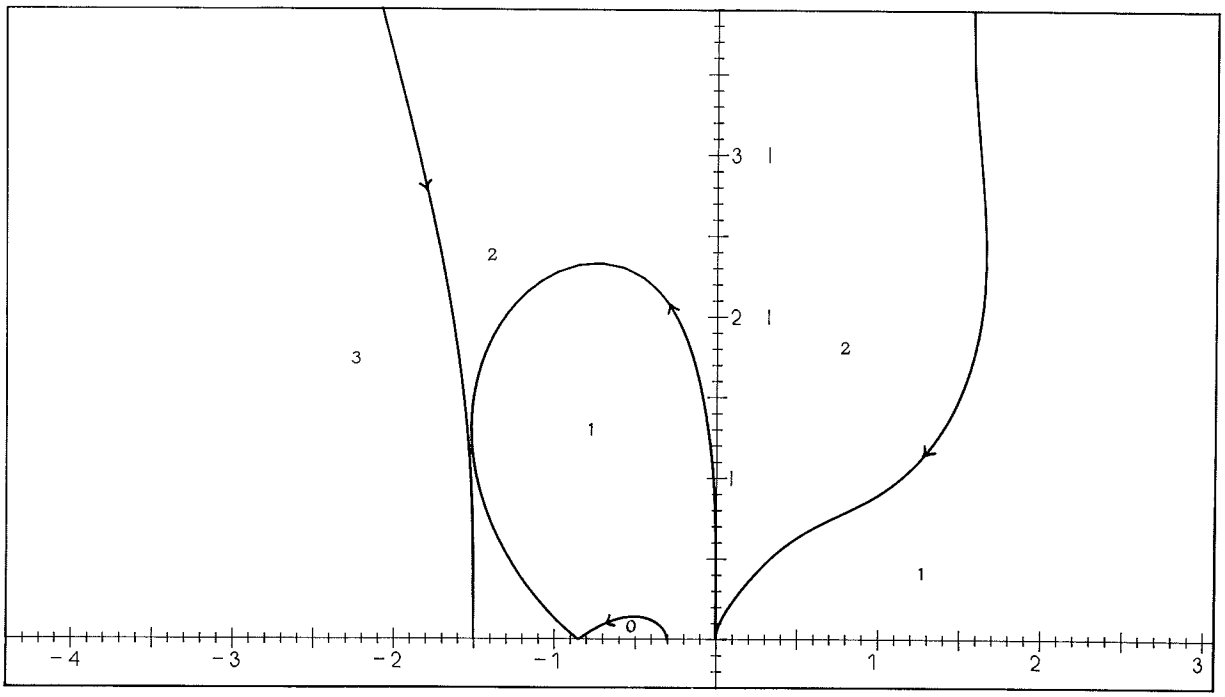

Fig. 7. Milne's method, PECE mode.

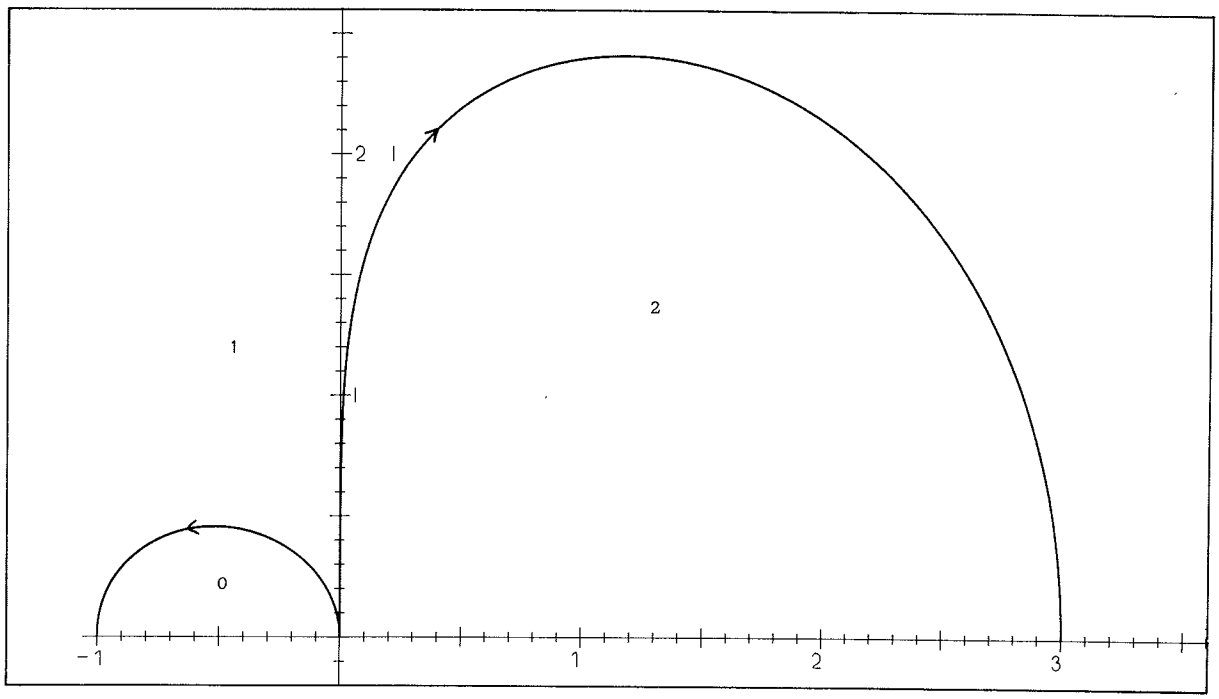

Fig. 8. Stetter-Simpson, PECE mode.

Boundary locus curves. The numbers indicate number of roots larger than 1 in each region.

not on the boundary of this region and Milne's method (in PECE mode) is therefore not to be recommended.

Stetter [28], [15, p. 101] has suggested the predictor

$$y_{n+2} + 4y_{n+1} - 5y_n = h \cdot (4f_{n+1} + 2f_n)$$

to be used together with Milne's corrector (Simpson's rule) in order to have a stable predictor-corrector method. The boundary locus curve for this method (in PECE mode) is shown in fig. 8. We have absolute stability in the almost circular region about (-1, 0).

The complicated behaviour of boundary locus curves for predictor-corrector methods is illustrated in fig. 9 - 12 for Hamming's method in modes $P(EC)^mE$, $m = 1, 2, 3, 4$ respectively.

We note that only part of the curves are shown, and that the straight line segments in figs. 11 and 12 (and on some later figures) are due to a too course step length in θ. As this happens away from the stability region we have not taken measures to remedy the situation. The numbers indicate the number of roots greater than one within each region. However, we are really not interested in the whole boundary locus curve, but only in the region of absolute stability. Therefore we shall from now on remove the unnecessary lines from the pictures and only show those parts that make up the boundary of the absolute stability region. This is <u>not</u> done automatically by the program, but requires human intervention. After having produced a first drawing of the boundary locus curve we determine the stability region by sampling the roots in the regions in question. We can then define a polygon in the $\bar{h}$-plane containing the stability region and only draw those (parts of) curves which are inside the polygon. We shall usually aim at polygons that are slightly larger than necessary in order to make it easier to distinguish between cusps on the boundary locus curve and intersections.

The absolute stability regions for Hamming's method in modes $P(EC)^mE$ for $m = 1, 2, 3, 4$ are shown in fig. 13. Those of the Adams-Bashforth-Moulton (ABM) method of order 4 in modes $P(EC)^mE$, $m = 1, 2, 3, 4$ are shown in fig. 14.

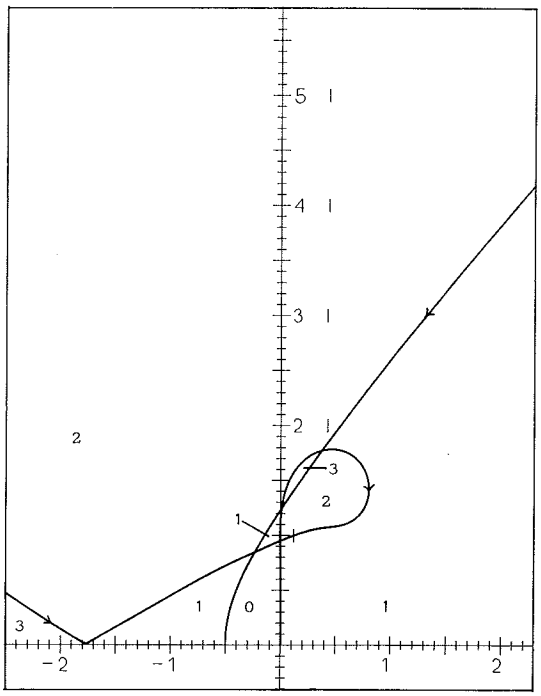

Fig. 9. m = 1.

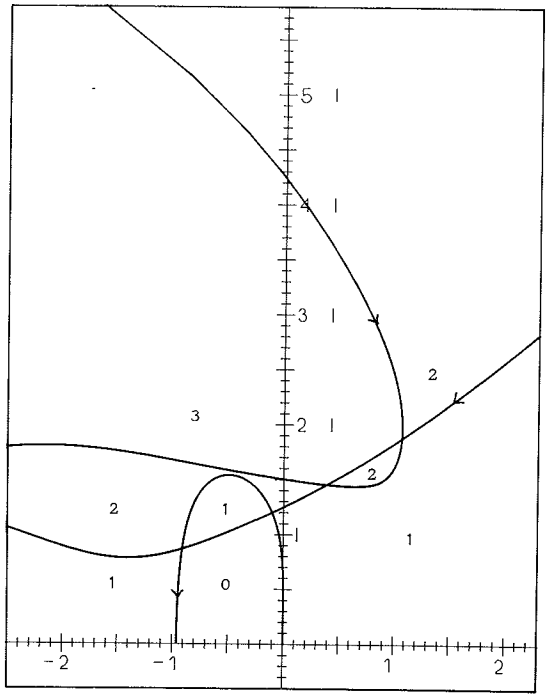

Fig. 10. m = 2.

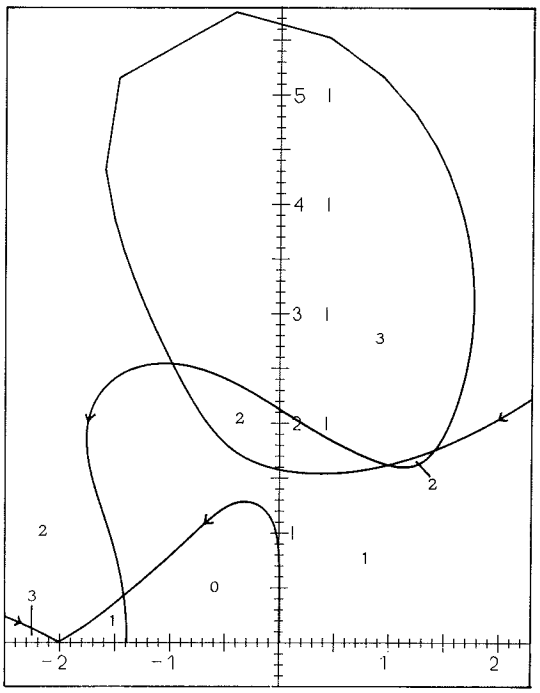

Fig. 11. m = 3.

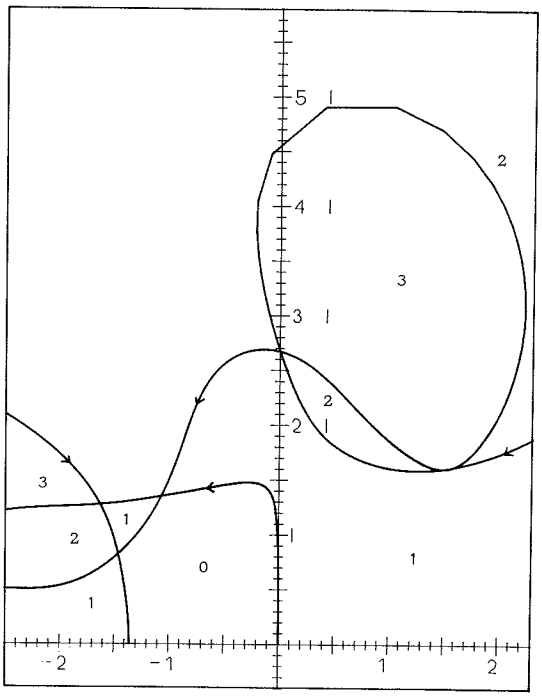

Fig. 12. m = 4.

Boundary locus curves for Hamming's method in modes $P(EC)^mE$. The numbers indicate number of roots larger than 1 in each region.

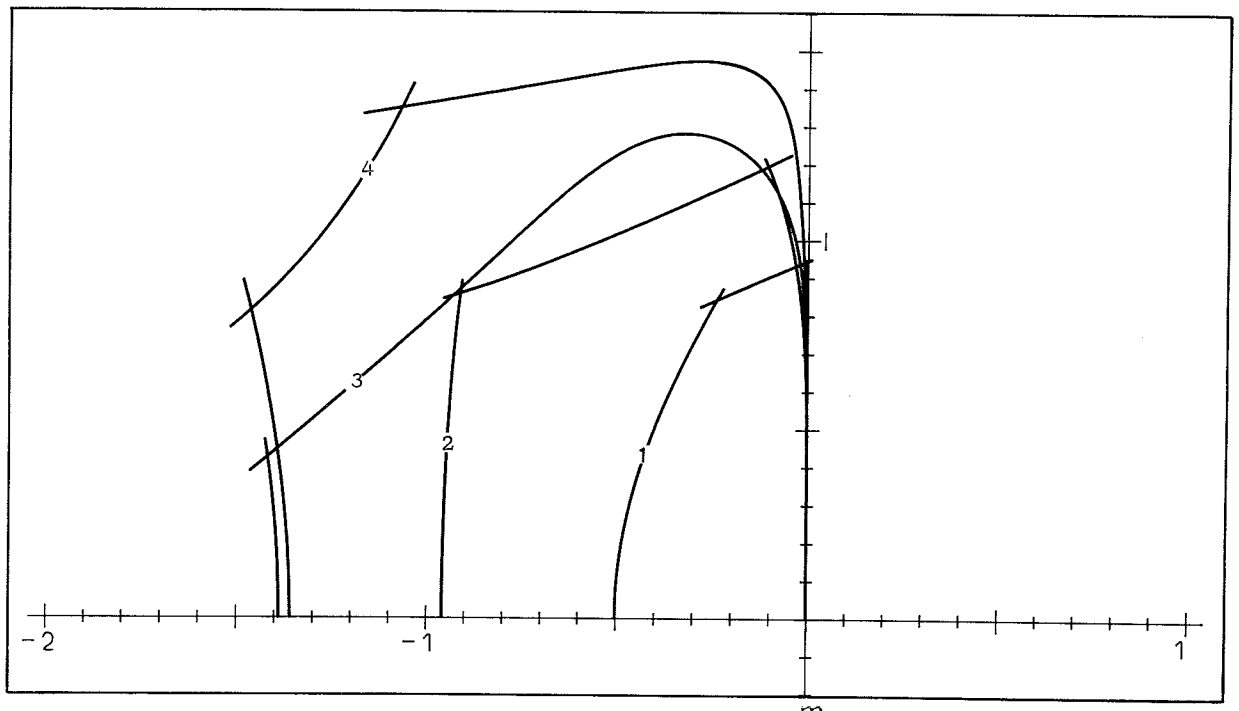

Fig. 13. Hamming, $P(EC)^mE$.

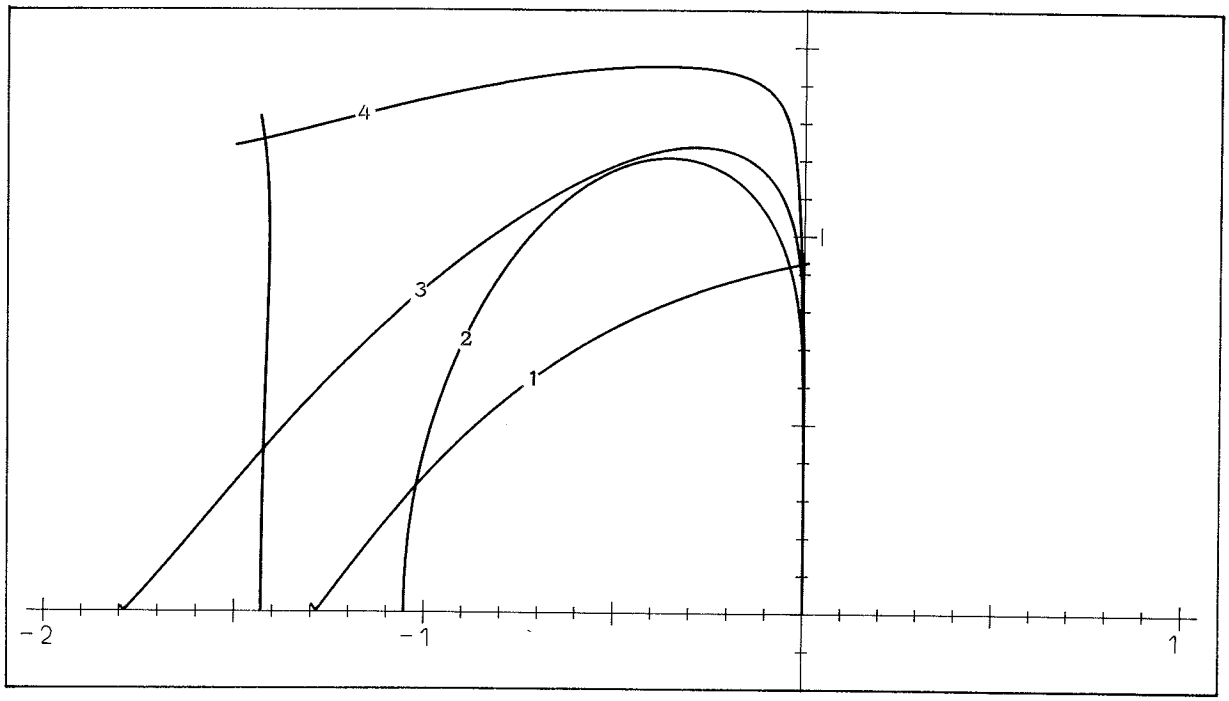

Fig. 14. ABM, p = 4, $P(EC)^mE$.

Stability regions for modes $P(EC)^mE$, m = 1, 2, 3, 4. The numbers indicate the value of m.

It is seen in these examples that correcting more than once by and large increases the stability region. It is often argued that correcting to convergence ($m \to \infty$) will get us to the stability region of the corrector. This is not the case for low order formulae where the introduction of the factor $M_m(\bar{h})$ sets an upper limit at $|\bar{h}| = 1/\beta_k$. This is seen on the cover where we give the boundary locus curves of the fourth order ABM method in modes $P(EC)^mE$, $m = 5, 6, 7, 8$. $M_m(\bar{h}) = -1$ at the cusp of each of the heart-shaped regions, and the stability region cannot extend this far. For ABM methods of order $p > 4$ the assertion seems to be true, however. As p increases $1/\beta_k$ increases slowly and the stability region of the corrector decreases and becomes the critical factor. This is illustrated in figs. 15 and 16 where we show the stability regions for the sixth order ABM method in $P(EC)^mE$ modes for $m = 1, 2, 3, 4$ (fig. 15) and $m = 5, 6, 7, 8$ (fig. 16). We notice that for $m = 4, 5$ and 6 the stability region actually stretches out further than that of the corrector (cf. fig. 5) in certain directions and that we for $m = 8$ have an almost identical stability region.

We stress the fact that because of the number of function evaluations, which is usually taken as the measure of computational complexity for predictor-corrector methods, we cannot recommend correcting more than twice for reasons of efficiency. This is also the case for $P(EC)^m$ mode as illustrated in fig. 17 for the fourth order ABM method ($m = 1, 2, 3, 4$). We note that the stability region for $P(EC)^m$ mode is very similar to, although slightly smaller than, the region for $P(EC)^{m-1}E$ mode (cf. fig. 14).

The stability regions of the ABM methods of order 2 to 6 in PECE mode are shown in fig. 18. The stability regions for PEC mode turn out to be slightly smaller than those for PECM mode (see p. 24 for a discussion of modification after the corrector) and Hall has shown [12] that these are identical to those for the predictor alone of order one higher and they can be seen in fig. 3. This is quite remarkable when one remembers that the argument for including the corrector is its better stability properties. For PEC mode the situation is in fact worsened - an additional function evaluation is necessary for good stability.

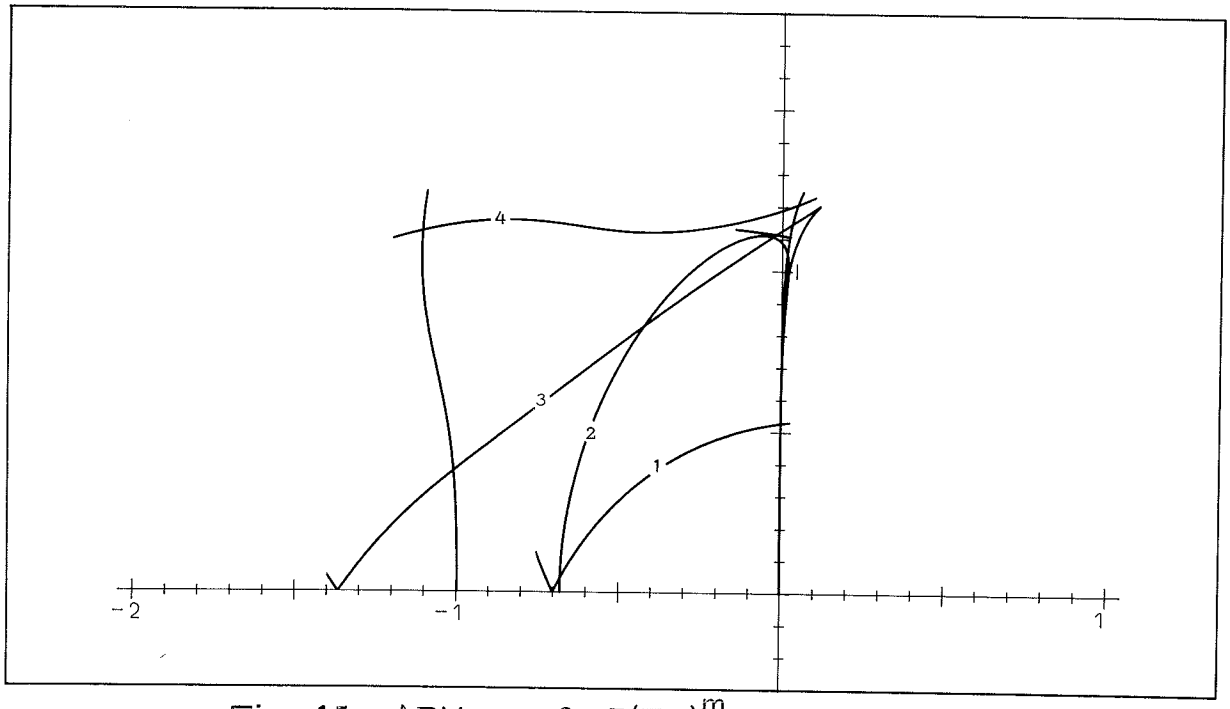

Fig. 15. ABM, p = 6, $P(EC)^mE$, m = 1, 2, 3, 4.

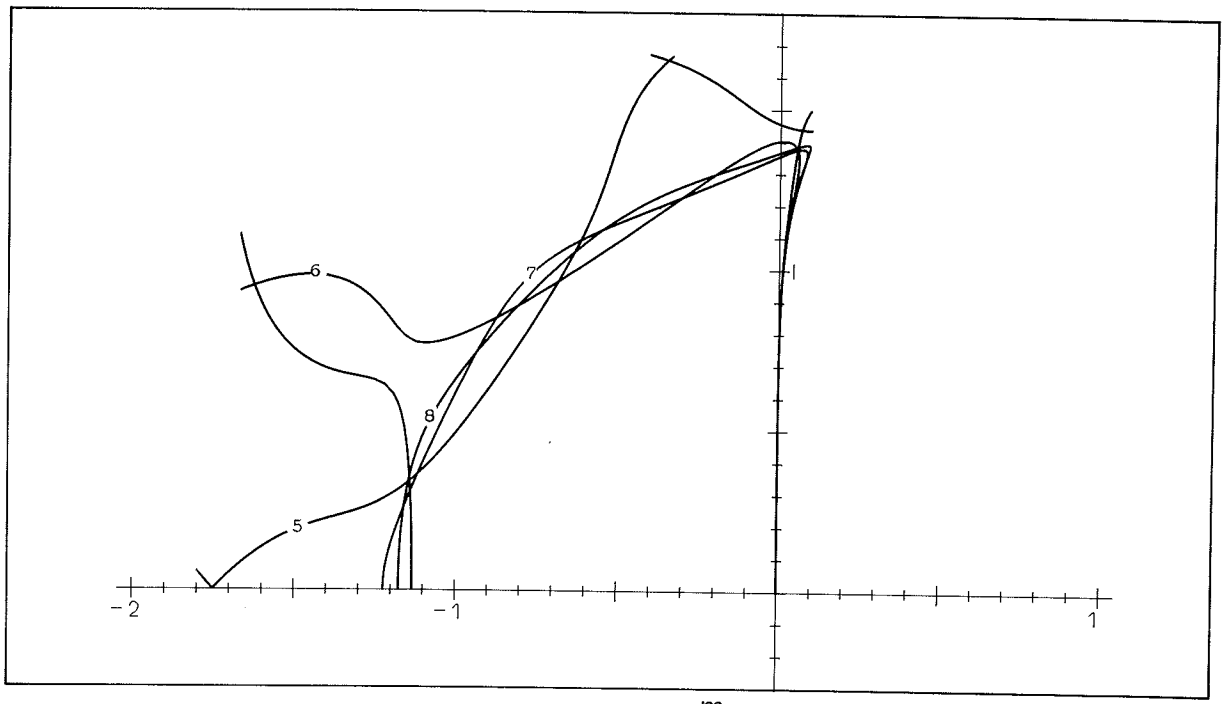

Fig. 16. ABM, p = 6, $P(EC)^mE$, m = 5, 6, 7, 8.

Stability regions for modes $P(EC)^mE$, m = 1-8. The numbers indicate the value of m.

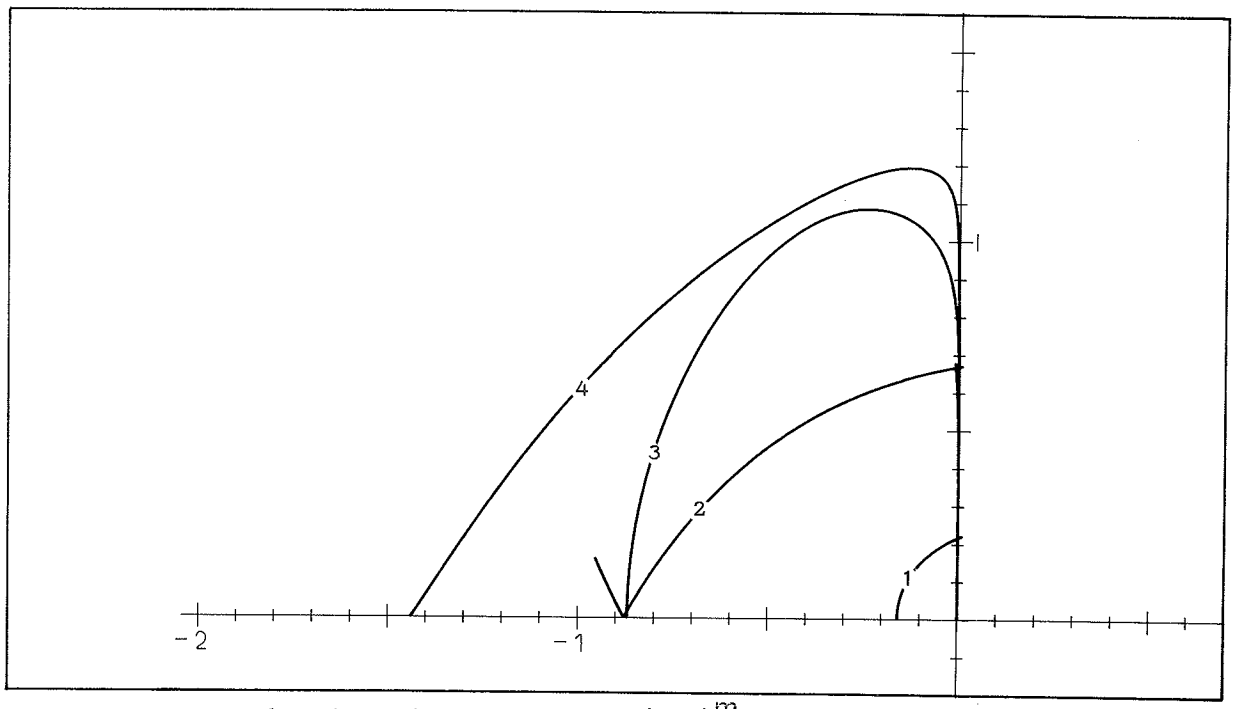

Fig. 17. ABM, p = 4, $P(EC)^m$, m = 1, 2, 3, 4.

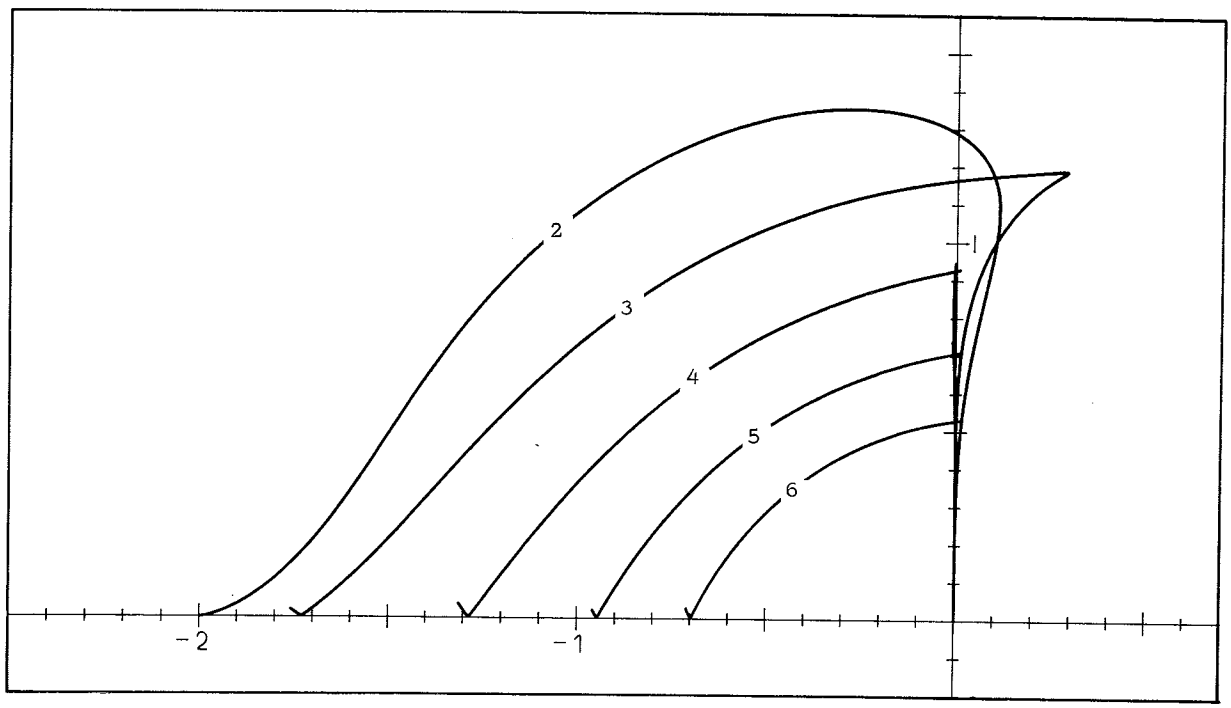

Fig. 18. ABM, PECE, p = 2, 3, 4, 5, 6.

Stability regions. The numbers indicate the values of m and p respectively.

5. Predictor-Modifier-Corrector Methods

When solving non-stiff problems with predictor-corrector methods it is often worthwhile to modify the predicted value before the function evaluation and the correction. This was in fact noted already by Milne [18, p. 65]. In the literature this is most often done by a modifier of the form

$$\hat{y}_{n+k} = y^*_{n+k} + \mu \cdot (y_{n+k-1} - y^*_{n+k-1}) \tag{6}$$

with

$$\mu = \frac{C^*_{p+1}}{C^*_{p+1} - C_{p+1}} \tag{7}$$

where C^*_{p+1} and C_{p+1} are the error constants of the predictor and the corrector respectively [15, p. 26 and 92], and the predictor and corrector have the same order, p. If $\alpha^*_j = \alpha_j$, $j = 0, 1, \ldots, k$ then the modifying term is a first order correct estimate of the local truncation error at the previous step, and we assume that this does not change much over one step.

If we look a little closer at the role of the predictor we notice that its main purpose is that of supplying a good starting value for the corrector iteration. Indeed, we would prefer to apply the corrector only once for the sake of efficiency. But in that case the ideal is not to compensate for the local truncation error of the predictor but rather to estimate the difference between the predicted and the corrected value. We are thus led to suggest the value $\mu = 1$ as a more reasonable choice. In practice the value of μ given by (7) is usually close to one as C^*_p is usually somewhat larger than C_p (and often of opposite sign) and the difference between the results from applying the two approaches will most often be insignificant. So maybe the best arguments for $\mu = 1$ are that the formulae are simpler and that we are no longer restricted to $p^* = p$ and $\alpha^*_j = \alpha_j$ $j = 0, 1, \ldots, k$.

In any case these considerations led us to investigating the stability properties of predictor-modifier-corrector methods with various modification factors, μ. The stability polynomials have been derived in [23, p. 73-74] using [29, p. 275 ff] and are for $PM(EC)^mE$ mode :

$$(8) \qquad \pi(z,\bar{h}) = z \cdot [\rho(z) - \bar{h}\sigma(z)] + M_m(\bar{h})(z-\mu)\ [\rho^*(z) - \bar{h}\sigma^*(z)]$$

and for $PM(EC)^m$ mode :

$$(9) \qquad \pi(z,\bar{h}) = \beta_k z^{k+1} [\rho(z) - \bar{h}\sigma(z)] + M_m(\bar{h})(z-\mu) \cdot [\rho^*(z)\sigma(z) - \rho(z)\sigma^*(z)]$$

where M_m is given by (4).

Fig. 19 shows the absolute stability regions of the third order ABM method in PMECE mode with $\mu = 0,\ 1/2,\ 9/10,\ 1,\ 3/2$. There is no particular interest connected with $\mu = 1/2$ or $3/2$ but we have included these values to show the general trend that the stability region for 3rd order ABM diminishes with increasing modification factor. In fig. 20 we are considering $PM(EC)^2E$ mode and the trend is the same although less pronounced. We remark that the use of modifier should be restricted to non-stiff problems, where the truncation error rather than stability limits the step-size. Fig. 21 is for PMECME mode where the second M indicates the use of Milne's device to improve the corrected value (see p. 24 and [15, p. 92]). Fig. 22 for Hamming's method in PMECE mode shows a slightly different picture. Looking at the real axis, the interval of absolute stability increases as μ increases from 0 through 1/2. The maximum interval is found for $\mu = .54$ and is $(-1.08, 0)$. From then on the trend is as for the Adams method shown. We are not advocating the use of 'under-modifying' but merely pointing out a curious effect.

Fig. 23 shows the effects of modifying and iterating the corrector for ABM, $p = 3$ in PECE, $P(EC)^2E$, $PM(EC)^2E$, PMECE and PEC modes ($\mu = 9/10$). They are listed here in order of decreasing stability interval. A similar picture is seen in fig. 24 for order 4. The picture for Hamming (fig. 25) is more confusing with $P(EC)^2E$-mode having the best stability properties but PMECE having almost as large a stability interval.

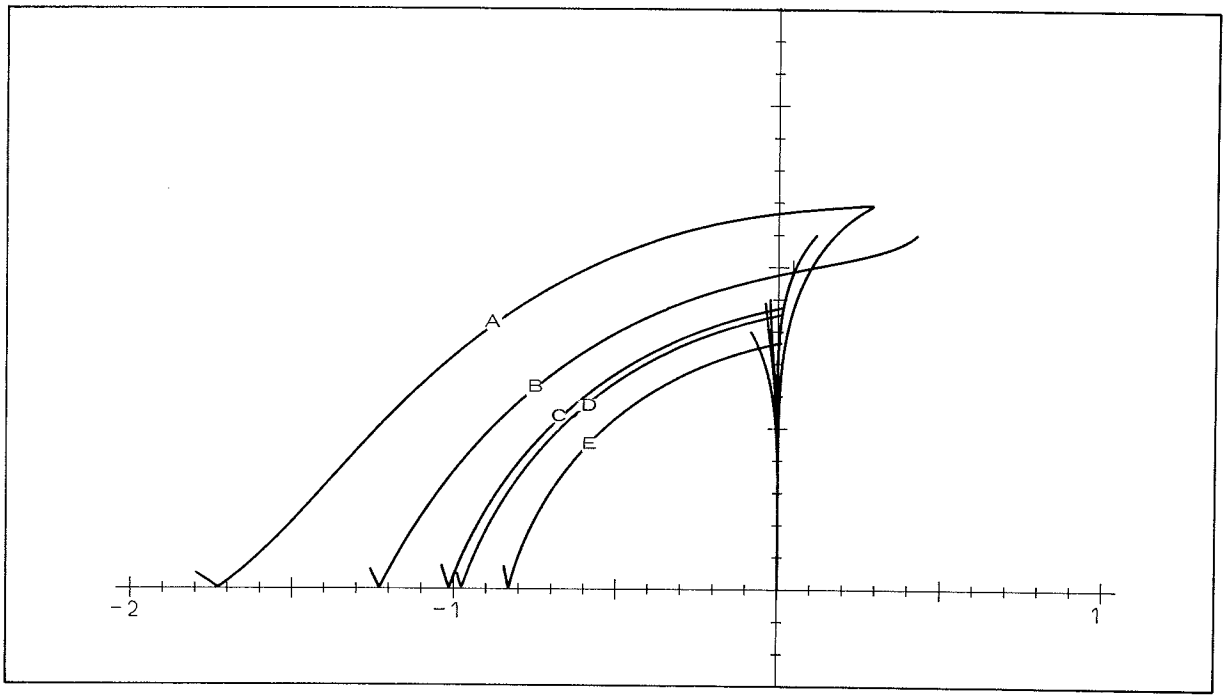

Fig. 19. ABM, p = 3, PMECE, μ = 0, 1/2, 9/10, 1, 3/2.

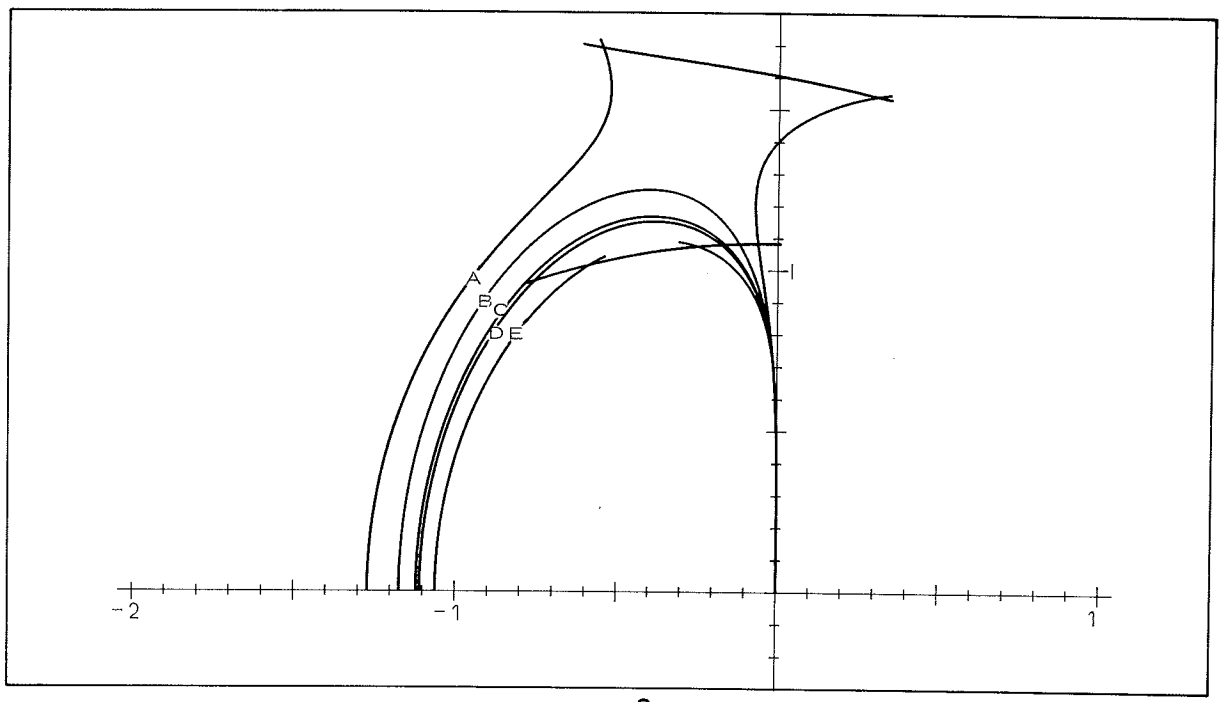

Fig. 20. ABM, p = 3, $PM(EC)^2E$, μ = 0, 1/2, 9/10, 1, 3/2.

Stability regions. The letters A, B, C, D, E indicate the various values of μ.

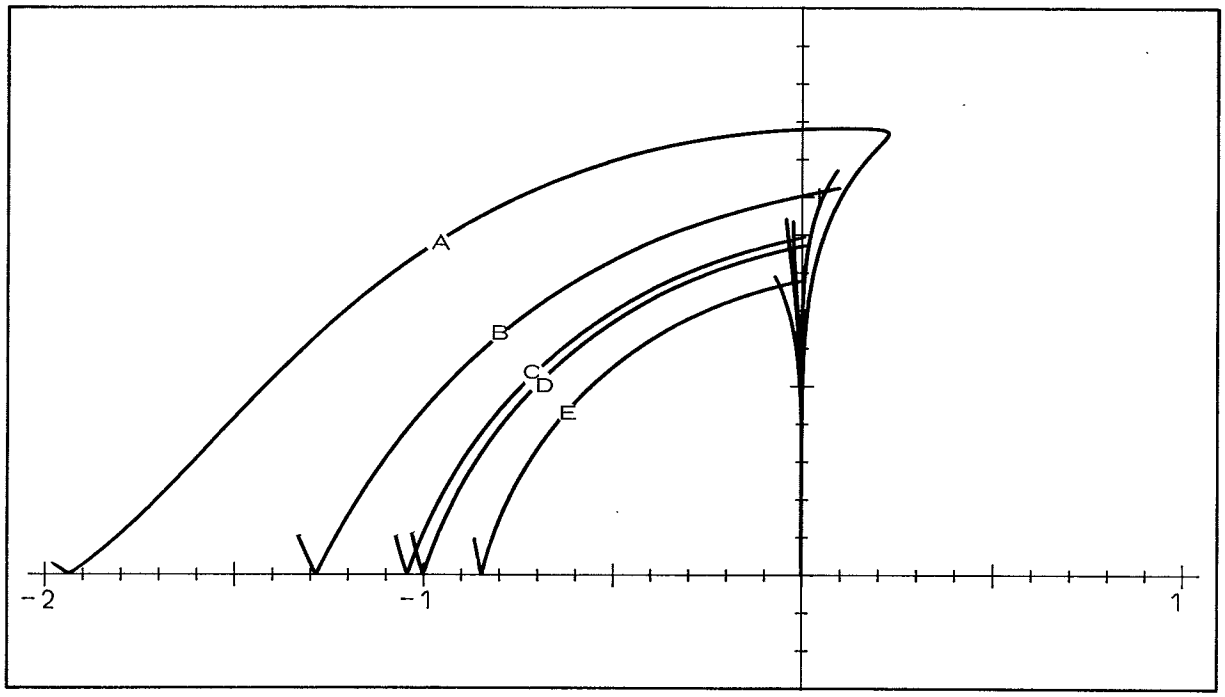

Fig. 21. ABM, p = 3, PMECME, μ = 0, 1/2, 9/10, 1, 3/2.

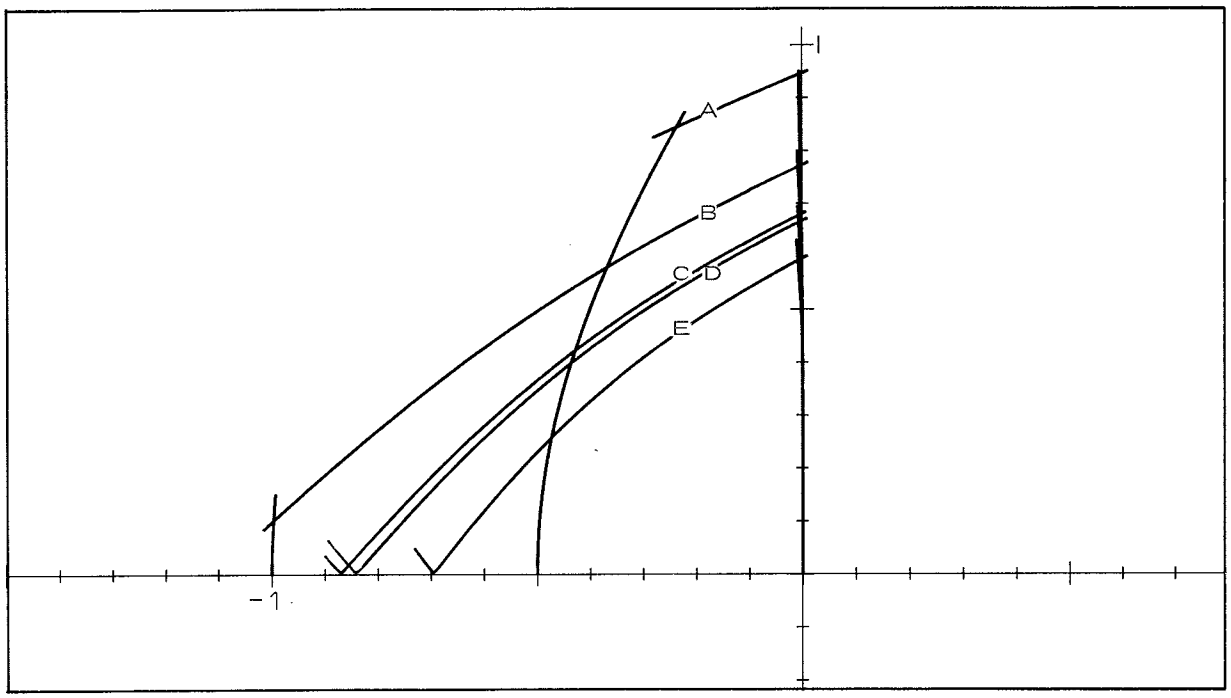

Fig. 22. Hamming, p = 4, PMECE, μ = 0, 1/2, 112/121, 1, 3/2.

Stability regions. The letters A, B, C, D, E indicate the various values of μ.

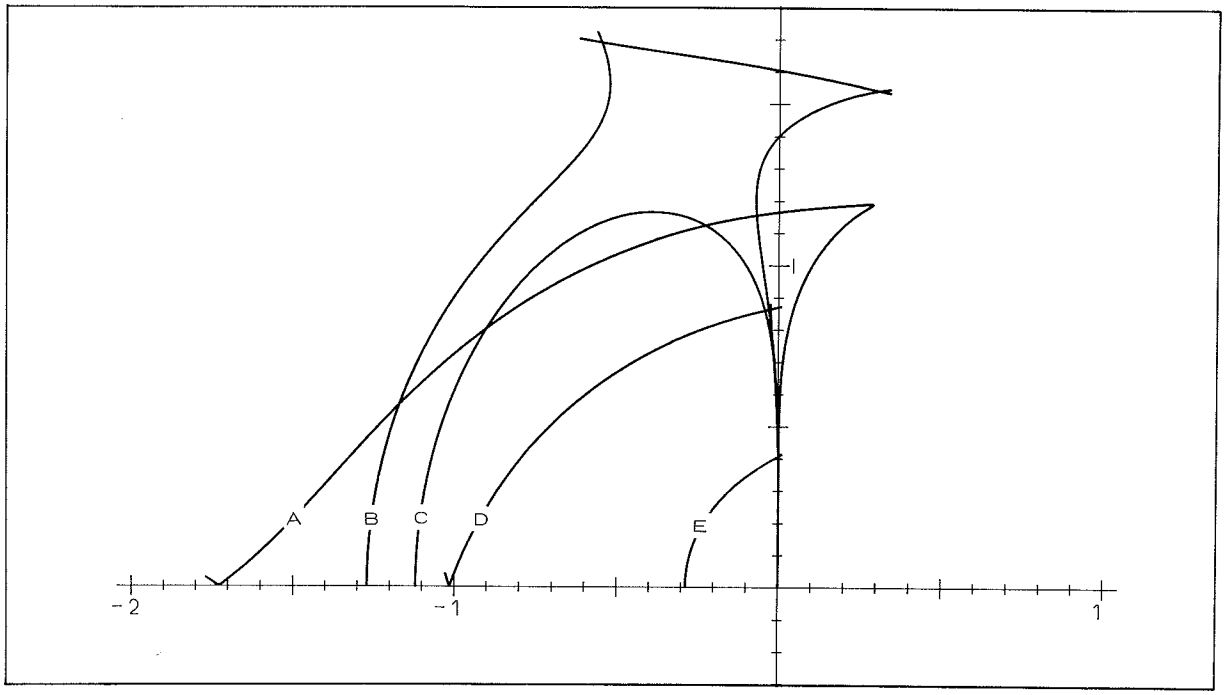

Fig. 23. ABM, p = 3.

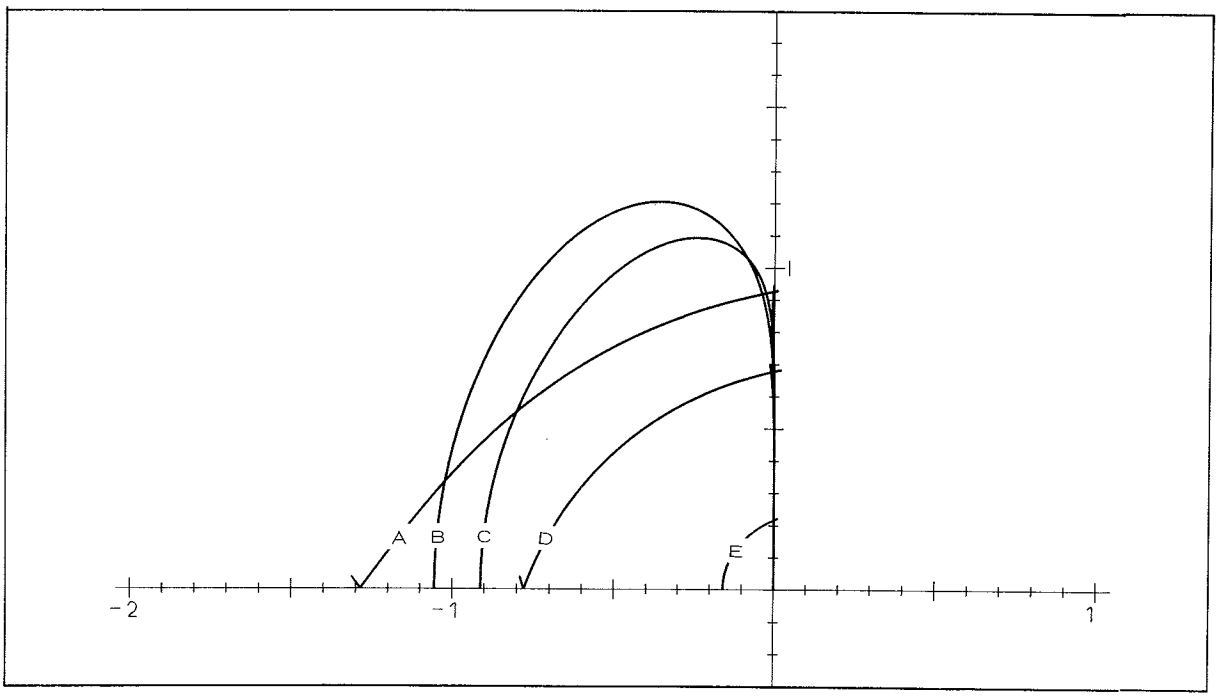

Fig. 24. ABM, p = 4.

Stability regions for modes PECE, $P(EC)^2E$, $PM(EC)^2E$, PMECE and PEC indicated by letters A, B, C, D, E, respectively.

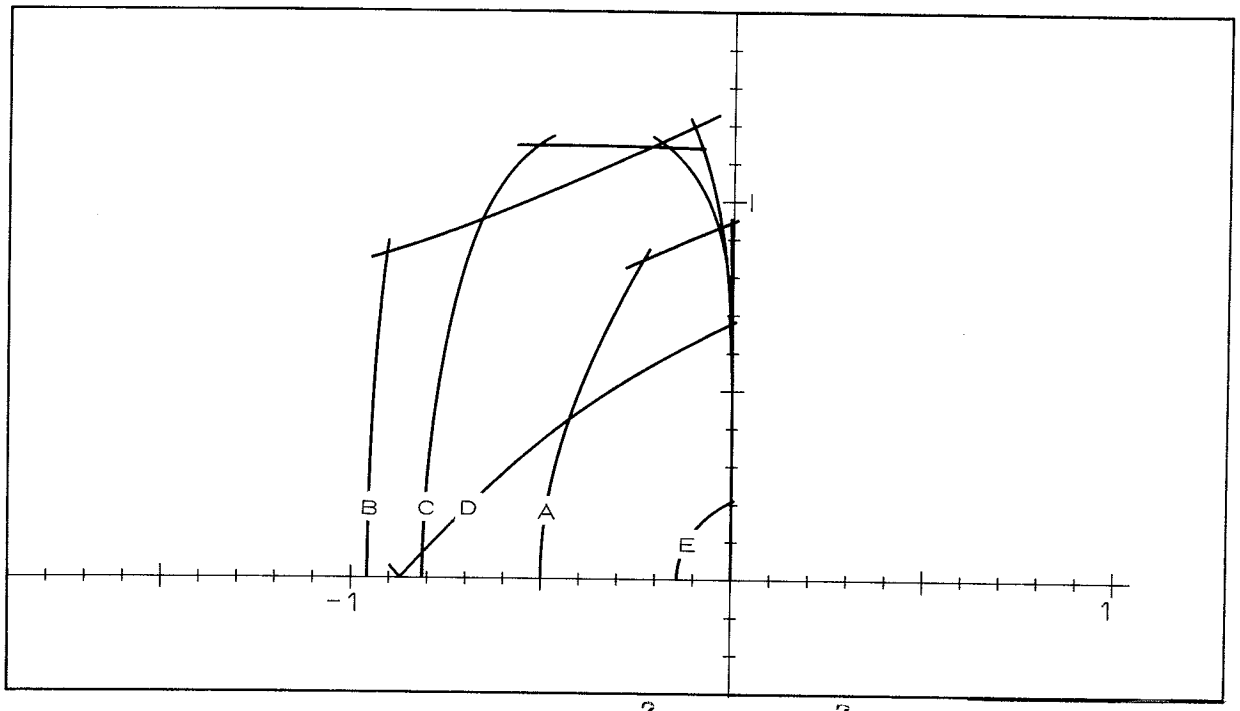

Fig. 25. Hamming, PECE, $P(EC)^2E$, $PM(EC)^2E$, PMECE, PEC.

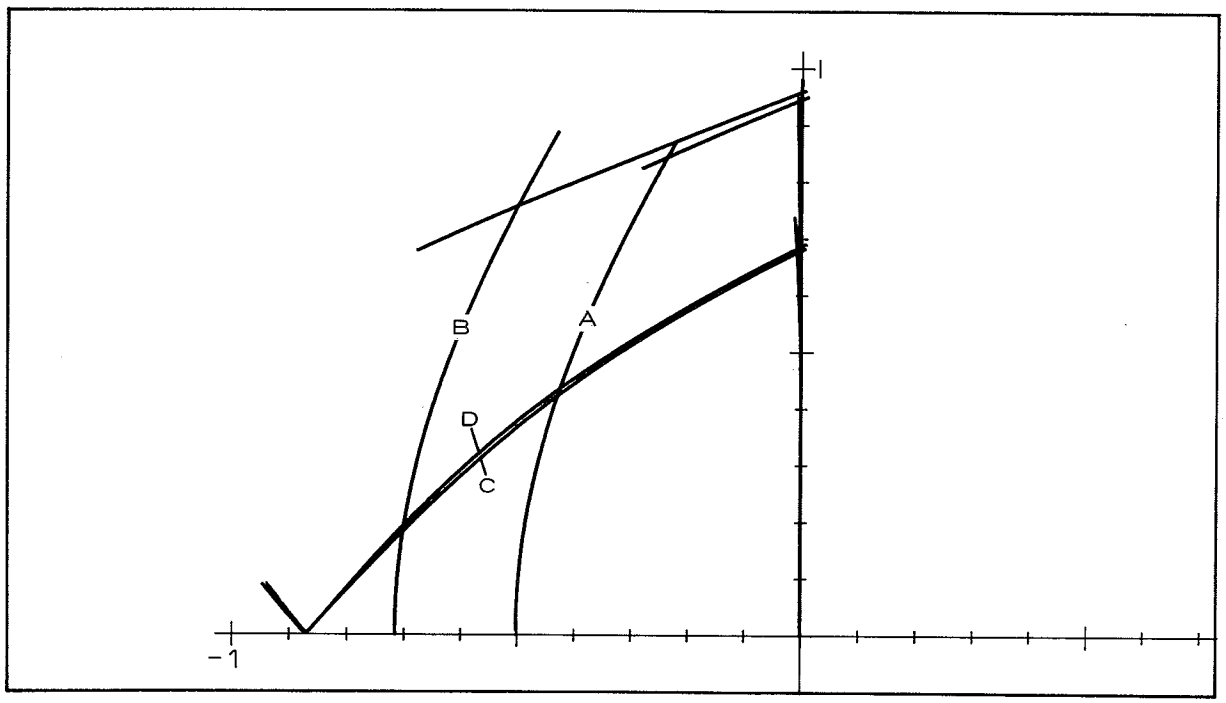

Fig. 26. Hamming, PECE, PECME, PMECE, PMECME.

Stability regions. The letters A, B, C, D (and E) indicate the various modes.

In fig. 26 we stay with Hamming but now in modes PECE, PECME, PMECE and PMECME. The modification after the corrector is meant to compensate for the local truncation error of the corrector formula [15, p. 94]. As has been pointed out by Shampine [26] the modification term does not in general provide a first order correct estimate of the local truncation error for Hamming's method, but applying it (in PECME mode) is nevertheless equivalent to using a 5th order corrector (in PECE mode) and, as fig. 26 shows, the stability is improved.

The ABM methods satisfy $\alpha_j = \alpha_j^*$ implying that Milne's device provides a first order correct estimate of the local truncation error. We can therefore on a sound theoretical basis modify after the corrector which, for an ABM method of order p, is equivalent to applying an Adams-Moulton corrector of order p+1 (in PECE mode). As has been noted earlier [26], [27, p. 134] this improves on the stability for $p < 12$. We demonstrate this fact in fig. 27 showing modes PECME and PECE (p = 2) together with PECE and PMECE (p = 3) and in fig. 28 which is similar with all orders raised by one.

Fig. 29 shows the stability regions for ABM (p = 4) in modes PECE, PECME, PMECE and PMECME (just as fig. 26 for Hamming) and in fig. 30 we are comparing modes PEC, PECE, $P(EC)^2$, $PM(ECM)^2$ and $P(ECM)^2$, (p = 4), pursuing the investigations of Brown, Riley and Bennett [2, methods A, B, C, E, F]. Measurements on the plots give the following table of stability-intervals, which is a slight improvement of formula (74) in [15, p. 103].

PEC	(- 0.16, 0)
PECE	(- 1.28, 0)
$P(EC)^2$	(- 0.88, 0)
$PM(ECM)^2$	(- 0.65, 0)
$P(ECM)^2$	(- 0.95, 0)

We can add to this, that with two function evaluations the largest stability interval, (- 1.41, 0), is achieved using PECME mode, a mode not considered by Brown, Riley and Bennett.

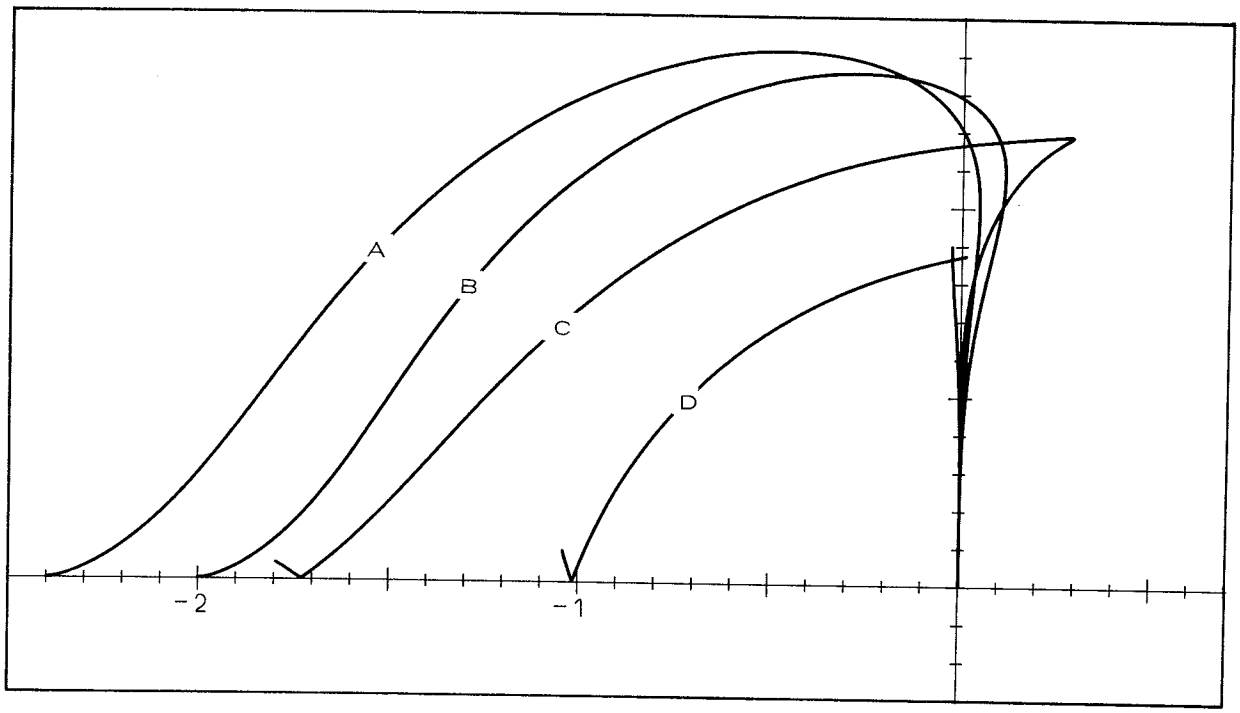

Fig. 27. ABM, p = 2 and 3.

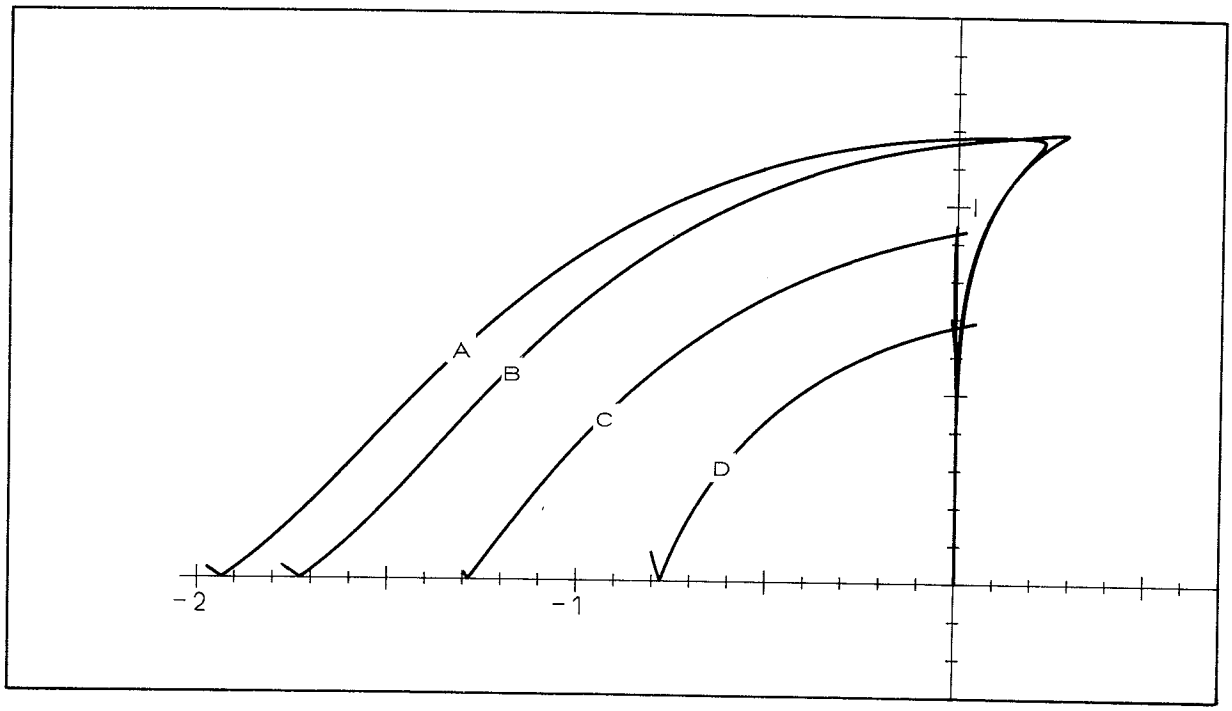

Fig. 28. ABM, p = 3 and 4.

Stability regions for modes PECME, PECE (low order) and PECE, PMECE (high order) indicated by letters A, B, C, D, respectively.

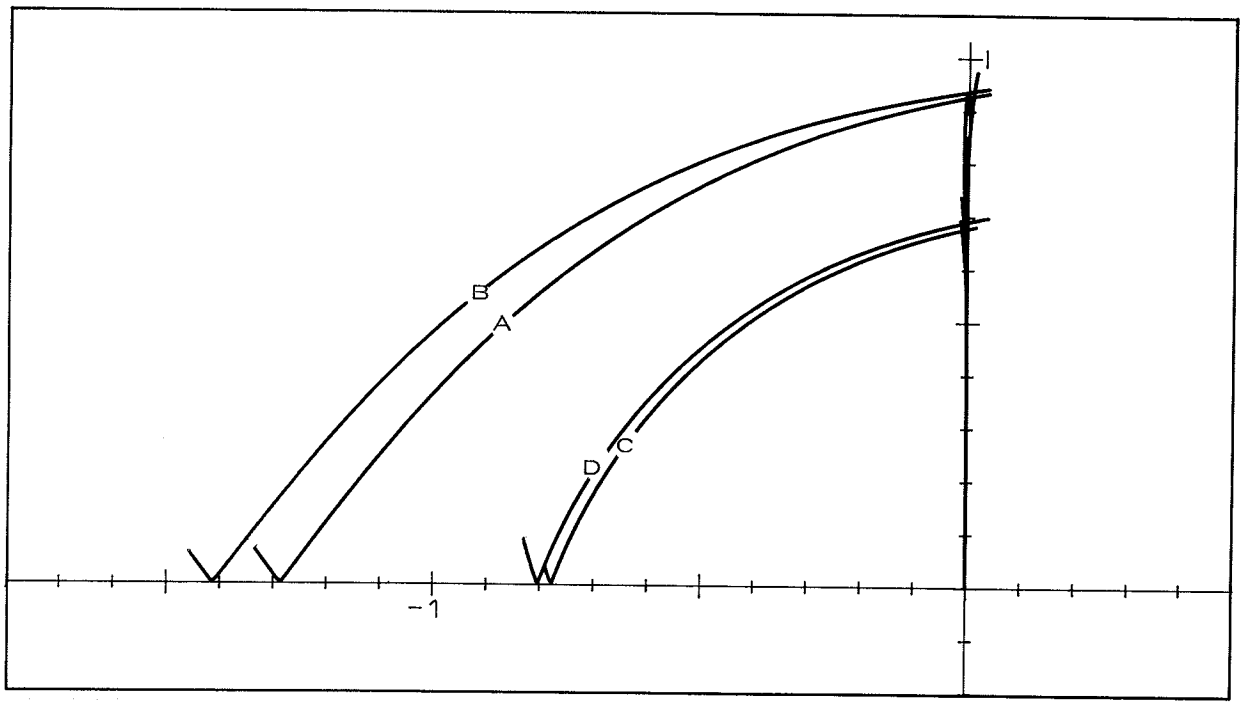

Fig. 29. ABM, p = 4, PECE, PECME, PMECE, PMECME.

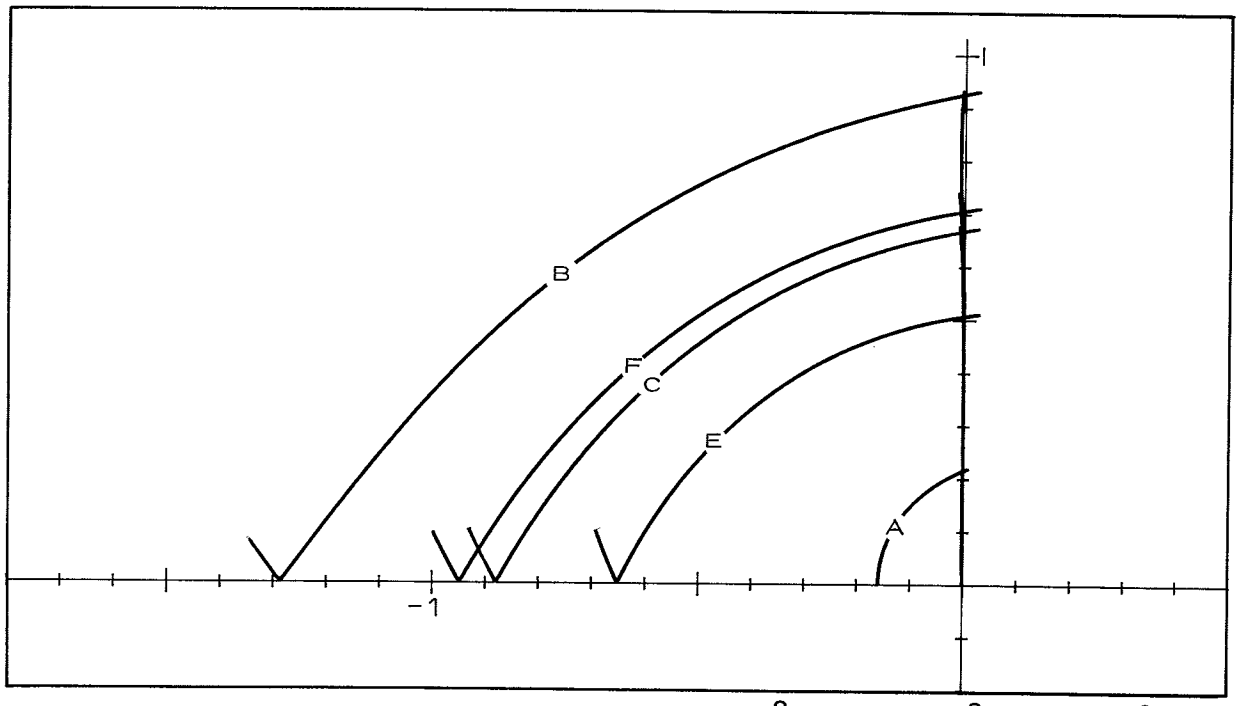

Fig. 30. ABM, p = 4, PEC, PECE, $P(EC)^2$, $PM(ECM)^2$, $P(ECM)^2$.

Stability regions. The letters A, B, C, D, resp. A, B, C, E, F, indicate the various modes.

6. Explicit Runge-Kutta Methods

An explicit, s-stage, Runge-Kutta method can be written as

$$(10) \qquad y_{n+1} = y_n + h \cdot \sum_{i=1}^{s} w_i k_i ,$$

$$(11) \qquad k_i = f(x_n + h\alpha_i,\ y_n + h \cdot \sum_{j=1}^{i-1} \beta_{ij} k_j) , \quad i = 1, 2, \ldots, s.$$

$$\alpha_1 = 0 ; \qquad \alpha_i = \sum_{j=1}^{i-1} \beta_{ij} , \qquad i = 2, 3, \ldots, s.$$

If this method is applied to the test equation, $y' = \lambda y$, we get

$$y_{n+1} = y_n \cdot P_s(\bar{h})$$

where P_s is a polynomial of order s. If $s \leq 4$ and the order of the method, $p = s$, then P_s coincides with the first terms in the power series for the exponential and thus all Runge-Kutta methods of the same order $p = s \leq 4$ have the same region of absolute stability. The familiar picture for $p = 1, 2, 3, 4$ is found in [15, p. 227] and also in fig. 31.

When $s > p$ the stability region may change and we have illustrated this in fig. 31 by also including Merson's 5-stage, 4th order method which is seen to have a larger stability region than the 4-stage 4th order methods.

This extra degree of freedom when $s > p$, which is forced upon us when $p > 4$, has been used to advantage by Lawson [16] who has tried to maximize the interval of stability for 6-stage 5th order methods, and also has recommended a formula with nice coefficients and reasonably close to the optimum. Unfortunately a misprint has sneaked into this formula [16, p. 597] where a closer examination and use of $\gamma = 1/2$ yields $k_3 = f(x_n + 1/4h,\ y_n + 1/16h(3k_1 + k_2))$.

Lambert [15, p. 143] cites the method and copies the error. Fig. 32 shows the stability region for Lawson's method, which has the stability interval $(-5.604, 0)$, together with those of Kutta-Nyström [19],

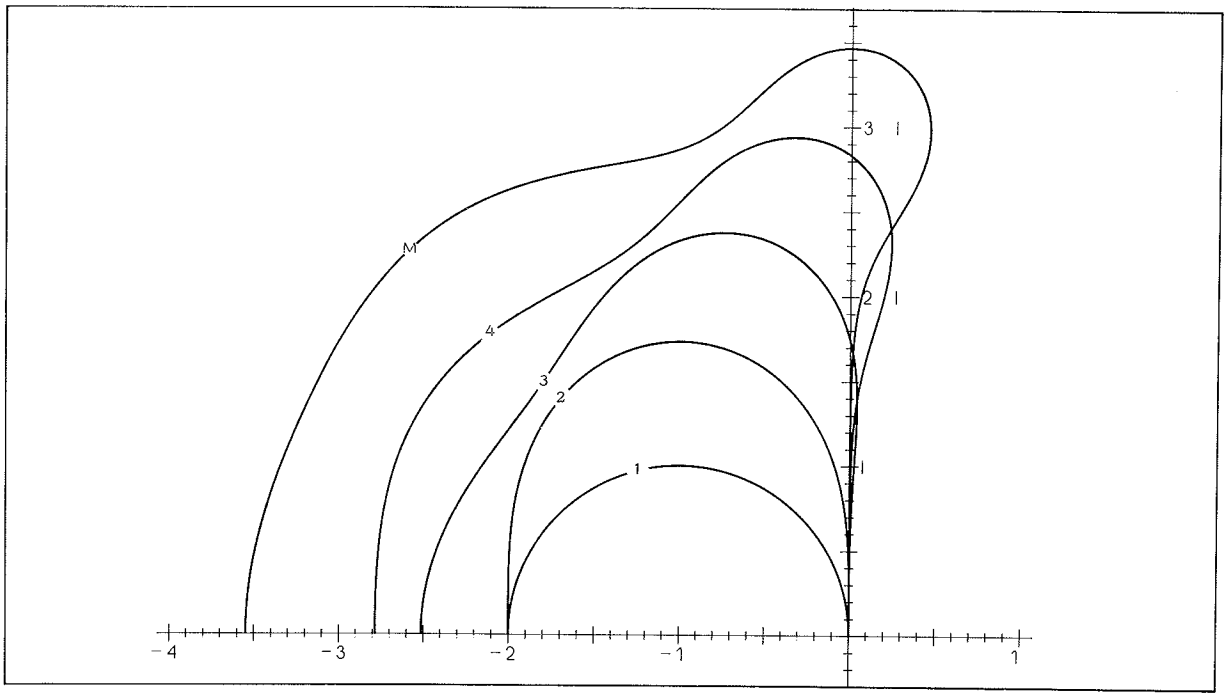

Fig. 31. Runge-Kutta, p = 1, 2, 3, 4 + Merson (indicated by M).

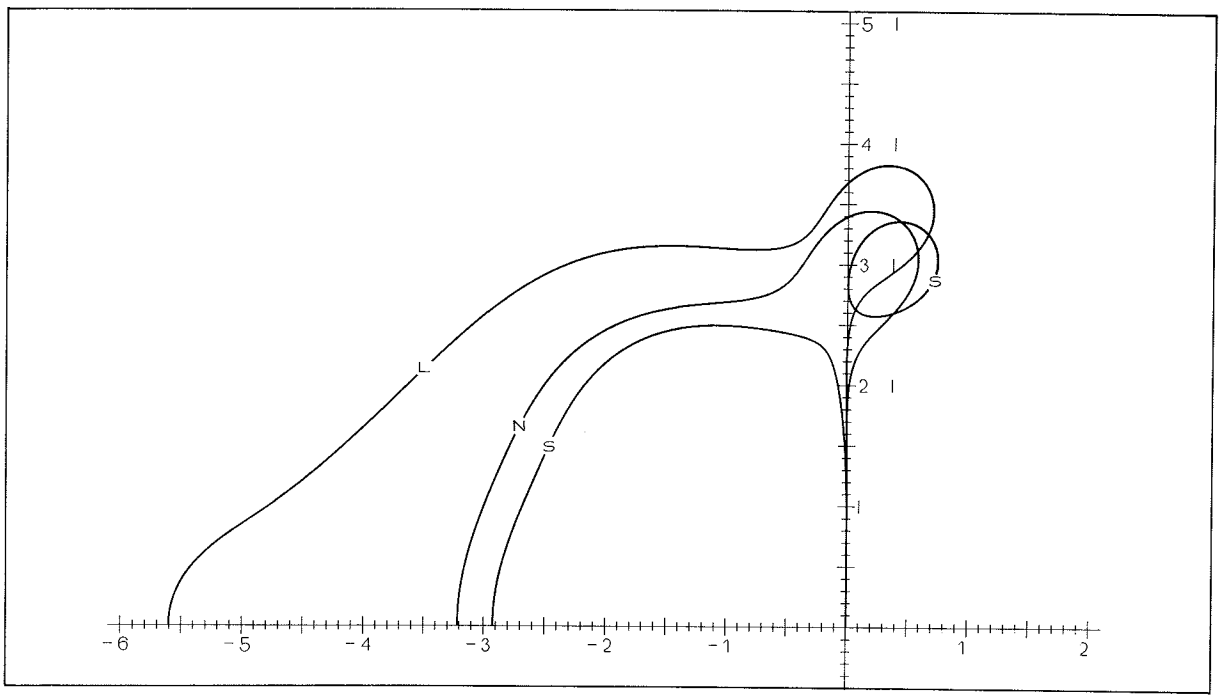

Fig. 32. Lawson (L), Scraton (S) and Kutta-Nyström (N).

Stability regions for explicit Runge-Kutta methods.

[15, p. 122] (s = 6 , p = 5) and Scraton [25], [15, p. 132] (s = 5 , p = 4). The latter is remarkable by having its stability set consisting of three disjoint regions in the complex plane. The two smaller regions, of which only the one with positive imaginary part is shown in fig. 32, are situated in the positive half plane where absolute stability is not a desirable feature.

7. Obrechkoff Methods

Obrechkoff methods [21] can be viewed as linear multistep methods that involve higher derivatives. Following the notation of Lambert [15, p. 199] a k-step Obrechkoff method using the first l derivatives may be written

$$(12) \qquad \sum_{j=0}^{k} \alpha_j y_{n+j} = \sum_{i=1}^{l} h^i \sum_{j=0}^{k} \beta_{ij} y_{n+j}^{(i)} , \qquad \alpha_k = 1 .$$

The stability theory can be generalized in a straightforward manner to these methods [15, p. 202], and the stability polynomial for the above method is

$$\sum_{j=0}^{k} (\alpha_j - \sum_{i=1}^{l} \bar{h}^i \beta_{ij}) z^j .$$

The boundary locus method can be applied with the complication (for $l > 1$) that the boundary locus may consist of several separate curves, a feature which we already saw in connection with (ordinary) predictor-corrector methods.

We shall confine ourselves to giving the boundary locus curves for four Obrechkoff methods. The first three are selected from [15, p. 201-202, formulae (6) - (8)] and shown in fig. 33. The implicit method (formula (6)) has a rather large stability region whereas the explicit methods have stability regions that are only slightly larger than for the corresponding 4th and 6th order AB-methods. The fourth method which is taken from [14, p. 173] shows some of the complications that may arise when there are more than one value of $\bar{h}$ corresponding to each θ. The arrows in fig. 34 show the direction of movement of the two $\bar{h}$-values, and the number of roots of the stability polynomial of magnitude larger than one in each region serve to illustrate the applicability of the right hand rule for these methods also.

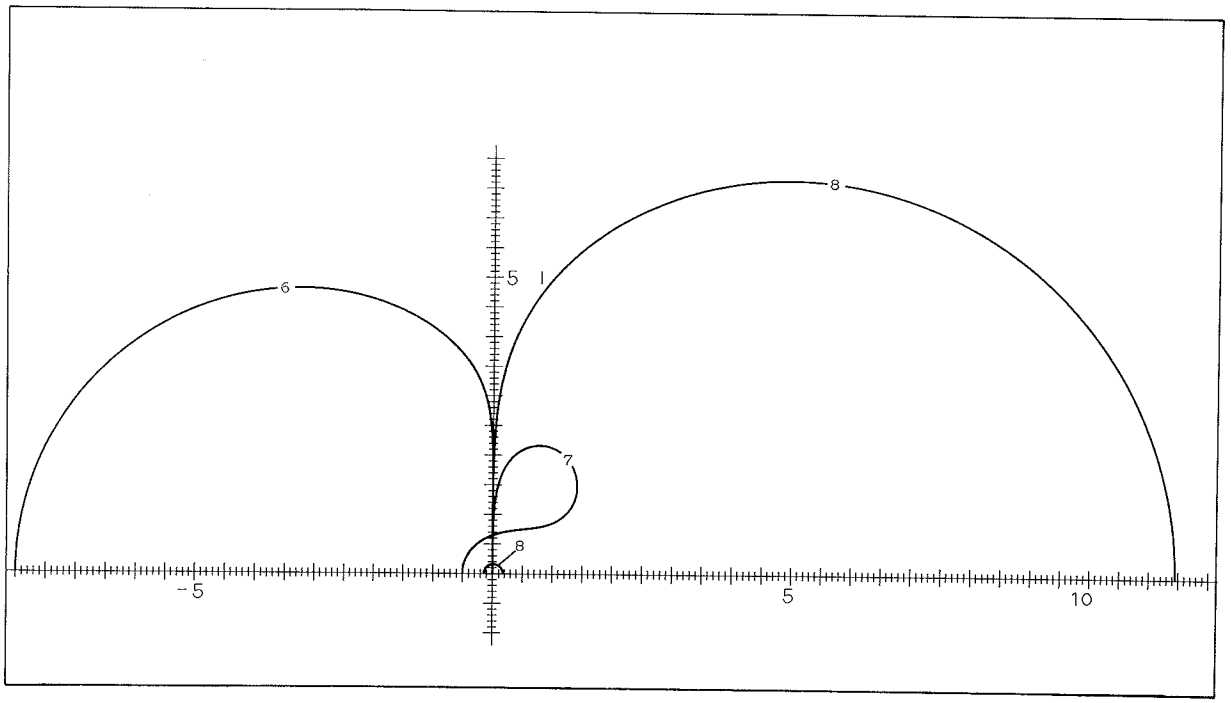

Fig. 33. Three Obrechkoff methods.

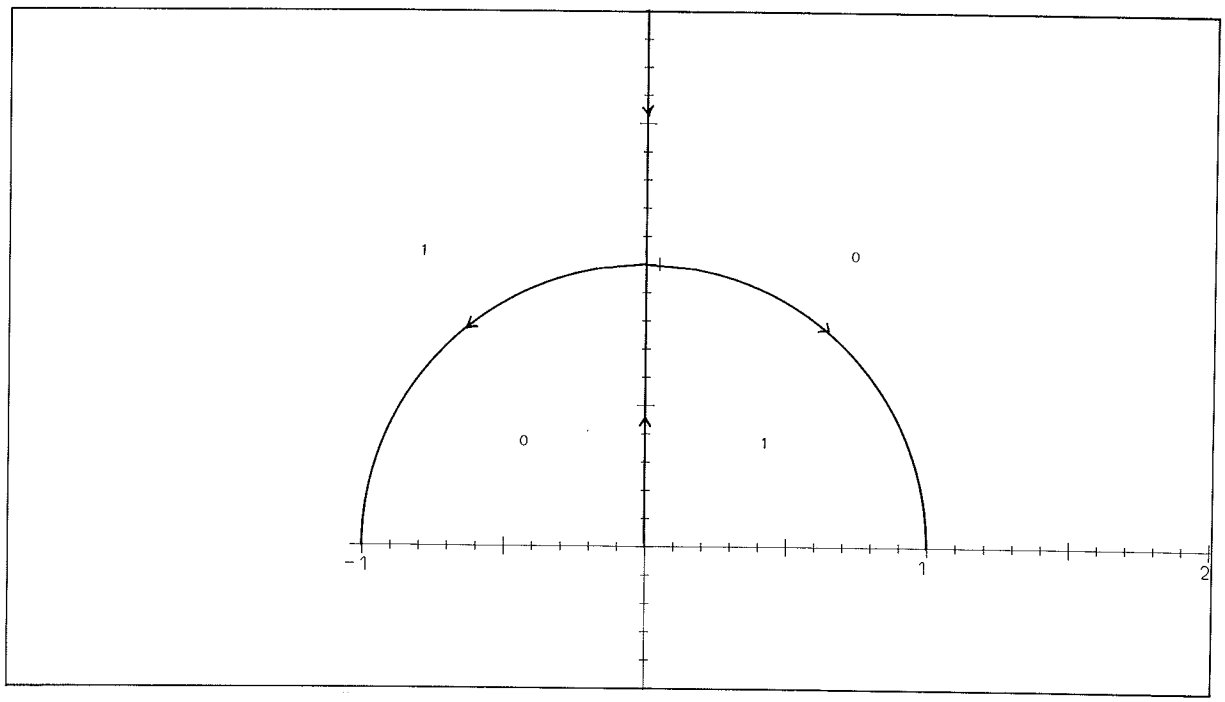

Fig. 34. Jeltsch's Obrechkoff method.

Boundary locus curves for selected Obrechkoff methods.

8. Stiff Problems

A system of q ordinary differential equations is called stiff if the Jacobian of the system, i.e. the matrix with coefficients $\frac{\partial f_i}{\partial y_j}$, has eigenvalues λ_k such that

$$Re(\lambda_k) < 0 \quad k = 1, 2, \ldots, q \quad \text{and}$$

$$Max(|Re\lambda_k|) \gg Min(|Re\lambda_k|) \quad k = 1, 2, \ldots, q.$$

Typical for the solution of a stiff problem is a short transient period with large variations and a long period (steady-state) with small variations. In the latter the step-size will be restricted by stability considerations unless one employs a method whose region of absolute stability covers a very large part of the left half-plane. Various stability concepts have been introduced with specific reference to stiff problems:

A-stability : The stability region contains the left half-plane [8].

$A(\alpha)$-stability : The stability region contains a wedge, $|arg(-\bar{h})| < \alpha$ [32].

A(0)-stability : $A(\alpha)$-stability for some $\alpha > 0$ [32].

A_0-stability : The stability region contains the negative real line [5].

Stiff stability : The stability region contains $\{\bar{h} \mid Re(\bar{h}) < 0\} \cap \{\bar{h} \mid Re(\bar{h}) < -a \text{ or } |Im(\bar{h})| < b\}$ for some $a, b > 0$ [11].

A closely related area of research is that of rational approximations, and in particular Padé approximations, to the exponential. So closely, indeed, that any rational approximation to the exponential can be produced by a suitable one-step Obrechkoff method. Corresponding to 'stability' we speak of acceptability of a rational approximation for a particular value of the independent variable if the magnitude of the rational expression is less than one. In particular we speak of A-, $A(\alpha)$-, and A_0-acceptability if the acceptability region contains the left half-plane, a wedge, or the negative real line.

9. Padé Approximations

Let $R_t^s(z) = \frac{P_s(z)}{Q_t(z)}$ be the (s, t) Padé approximation to exp(z) with s and t the degrees of the numerator and the denominator, respectively. It is clear that $R_t^s(z)$, for $s > t$, cannot be acceptable at infinity and therefore not even A_0-acceptable. Birkhoff and Varga [1] proved that $R_t^s(z)$ is A-acceptable for t = s (we denote these the diagonal Padé approximations), and Ehle [10] showed the A-acceptability for t = s+1 and t = s+2. Ehle conjectured and Wanner, Hairer and Nørsett recently proved [31] that no other subdiagonal Padé approximations are A-acceptable, although they all are A_0-acceptable [30].

We give the boundary locus curves for the (0, t) Padé approximations (t = 1 - 6) in fig. 35. The approximations are acceptable 'outside' the curves. We note that for $t \geq 3$ the approximations are $A(\alpha)$-acceptable ($\alpha < \pi$). We also note that for $1 \leq t \leq 4$ the acceptability region is the mirror image of the interior of the complement of the stability region for the t-stage, t-th order Runge-Kutta method, a fact which follows easily from the observation that the stability polynomial for this method is the (t, 0) Padé approximation to the exponential.

Fig. 36 shows the (1, t) Padé approximations (t = 2 - 6) and fig. 37 the (2, t) Padé approximations (t = 3 - 6).

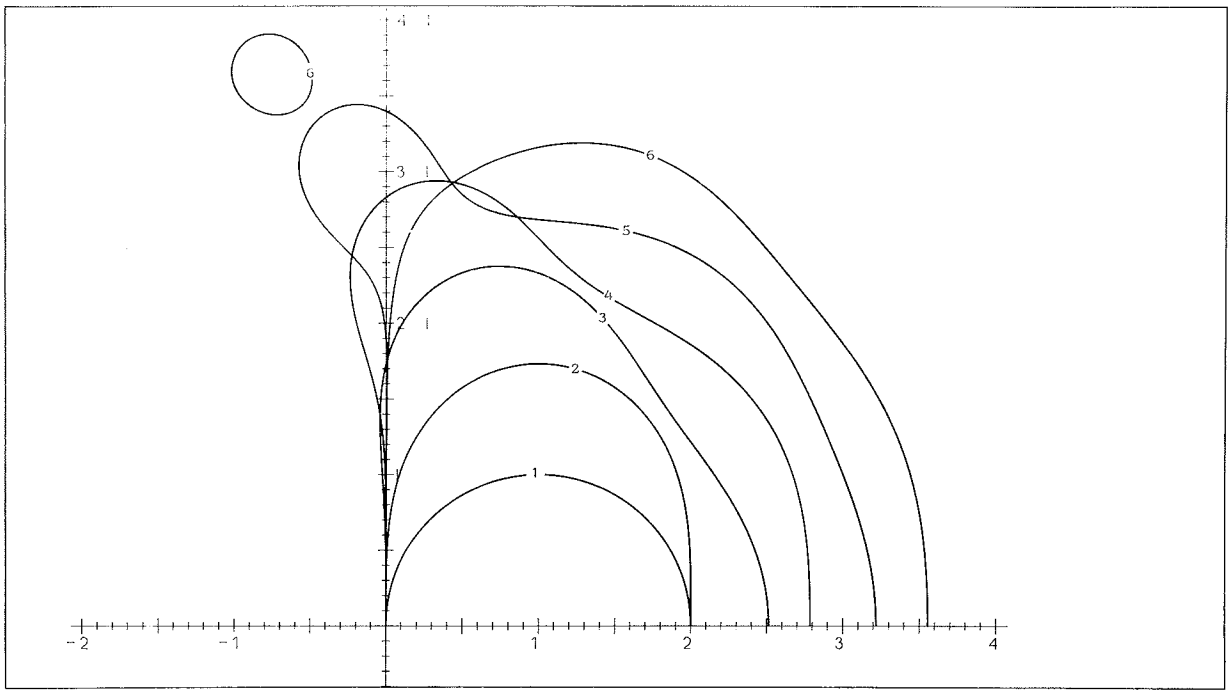

Fig. 35. Padé (0, t), t = 1, 2, 3, 4, 5, 6.

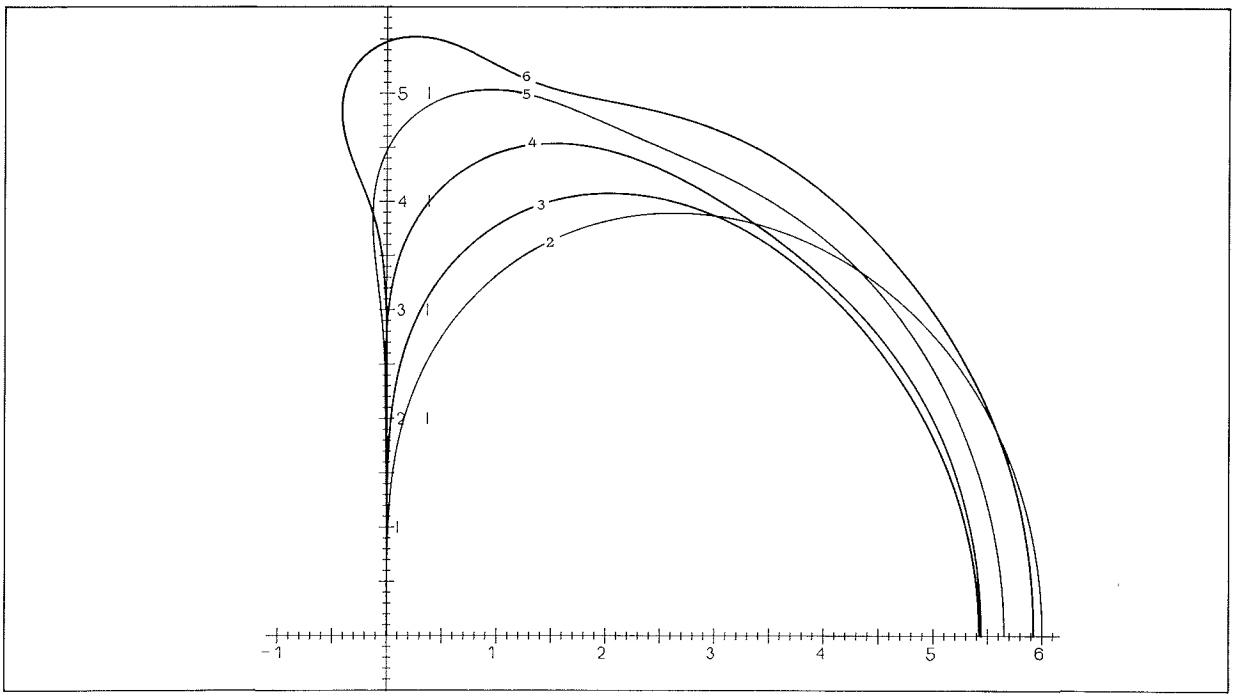

Fig. 36. Padé (1, t), t = 2, 3, 4, 5, 6.

Boundary locus curves for Padé approximations to the exponential.

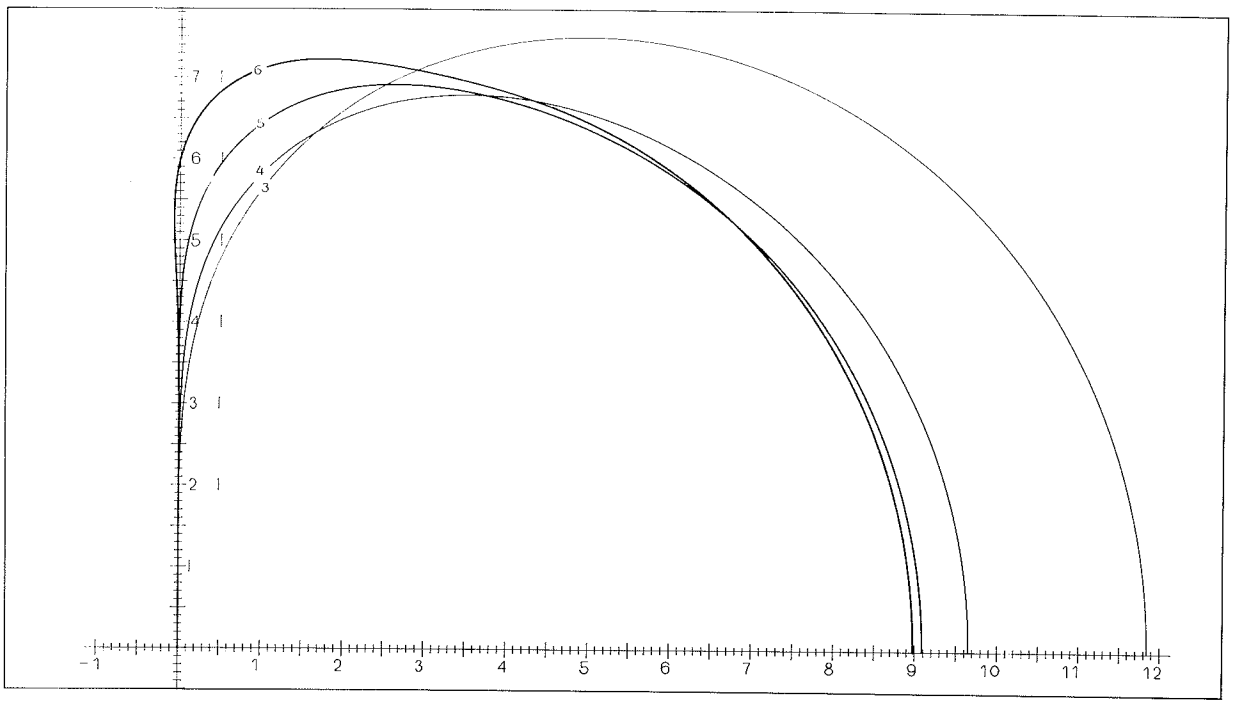

Fig. 37. Padé (2, t), t = 3, 4, 5, 6.

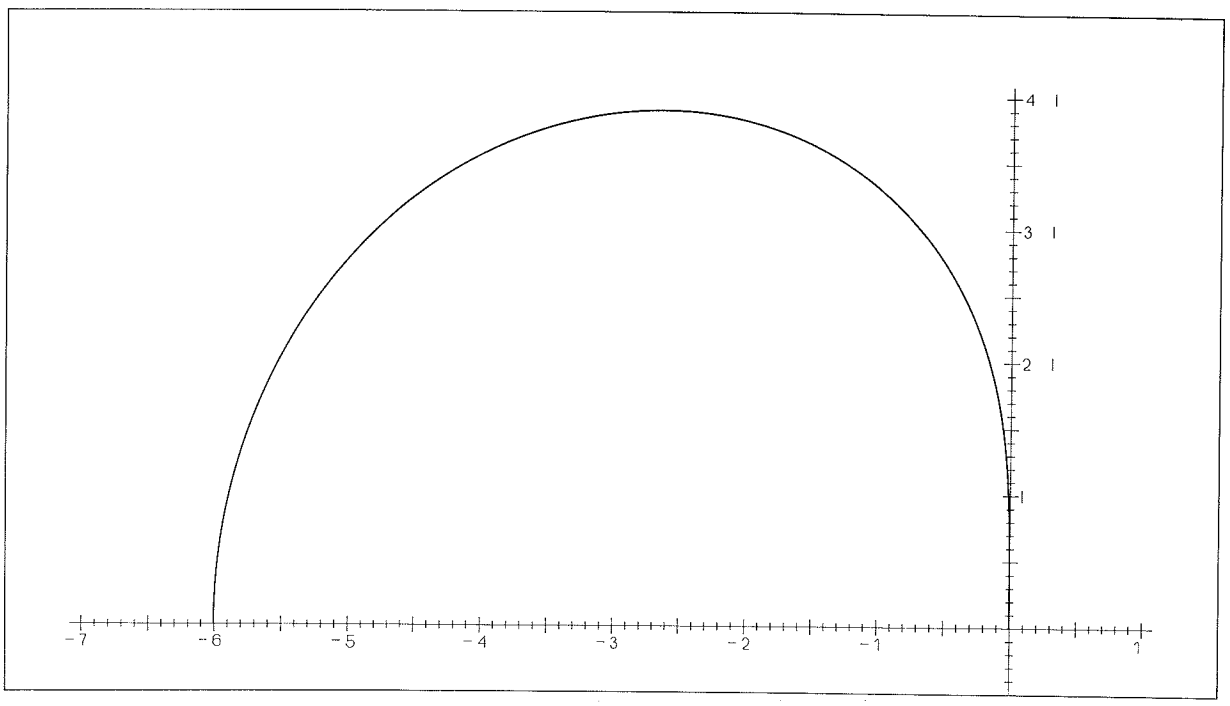

Fig. 38. Implicit Runge-Kutta, (Butcher, $\nu = 2$).

Boundary locus curves.

10. Implicit Runge-Kutta Formulae

With specific regard to stiff problems implicit Runge-Kutta formulae have been proposed, the implicitness referring to the definition of the k_i which in section 6 were given explicitly by the previous k_j. For the implicit formulae we have instead of formula (11) :

$$(13) \qquad k_i = f(x_n + h\alpha_i\ ,\ y_n + h \cdot \sum_{j=1}^{s} \beta_{ij} k_j) \qquad i = 1, 2, \ldots, s.$$

which means that a (large) system of (non-linear) equations must be solved in order to find the k_i. Despite such implementation problems implicit Runge-Kutta formulae can be quite useful because of good stability properties.

We supply in fig. 38 the (identical) stability regions of two methods suggested by Butcher [4, $\nu = 2$, table 1 and 2] which happen to be equivalent to the (2, 1) Padé approximation. Compare with the (1, 2) curve in fig. 36. In fig. 39 we show two other methods by Butcher [3, p. 51], [15, p. 160 and 154], one implicit with boundary locus curve equal to the imaginary axis, (it is equivalent to the (2, 2) Padé approximation) and one semi-implicit which is equivalent to the (3, 1) Padé approximation.

In fig. 40 we indicate the stability regions of three Rosenbrock methods, $R_{2,3}(u, \delta_i)$, $i = 1, 2, 3$, [33], one of them A-stable and the two others $A(\alpha)$-stable with $\alpha < \pi$.

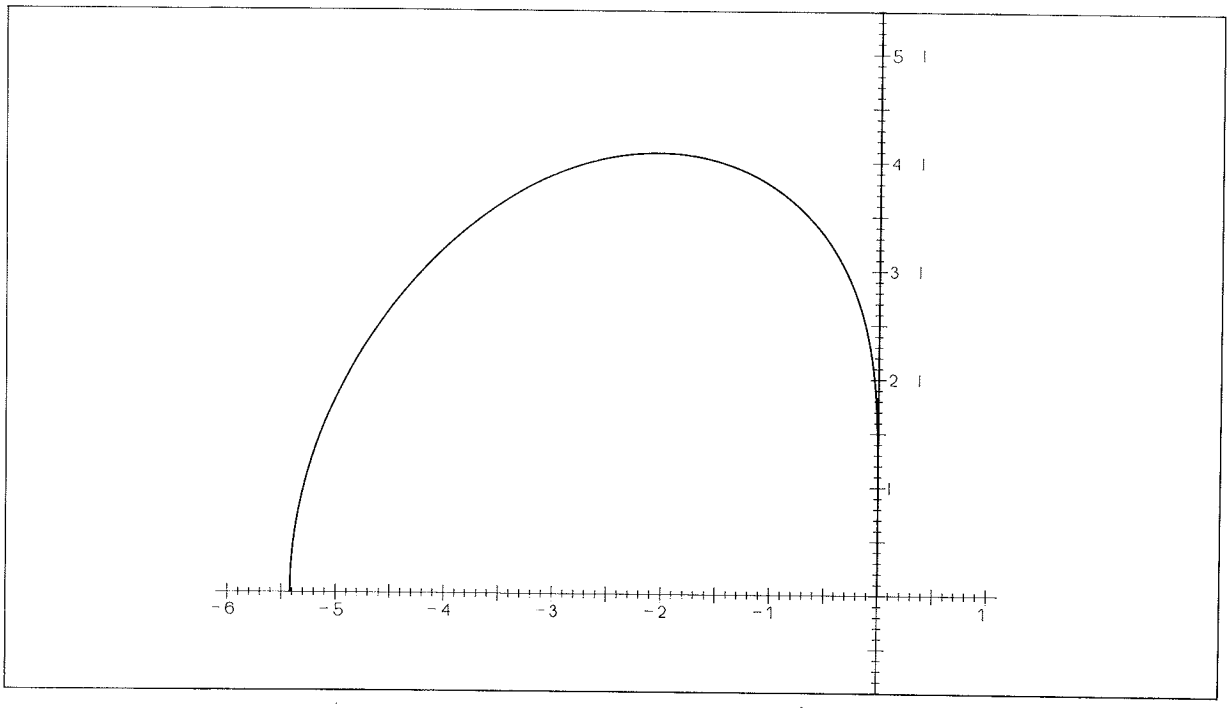

Fig. 39. Runge-Kutta formulae, (Butcher).

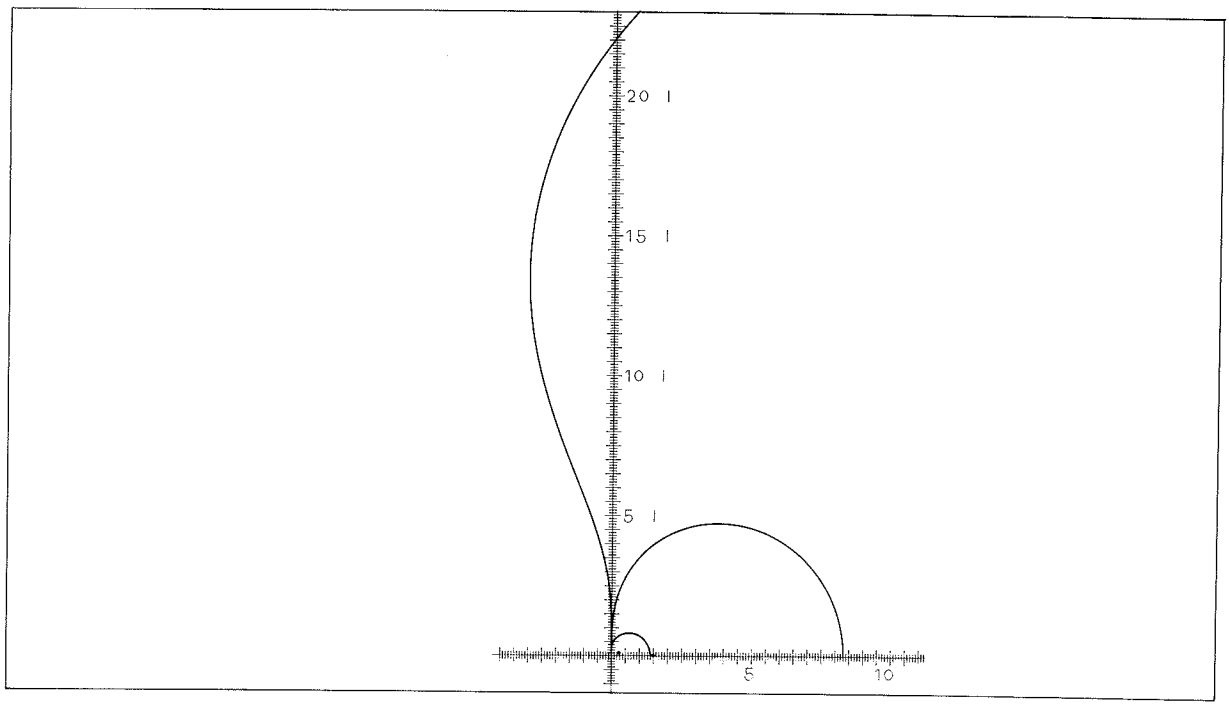

Fig. 40. Rosenbrock methods, $R_{2,3}(u, \delta_i)$, $i = 1, 2, 3$, (Wolfbrandt).

Stability regions.

11. Backward Differentiation Formulae

Among the linear multistep formulae the most popular ones for stiff problems are the backward differentiation formulae (BDF) [11], [15, p. 242]. In fig. 41 we show the boundary locus curves of the p step, p-th order BDF (p = 2, 3, 4, 5, 6). The stability region is the 'outside' of the curves, and all these BDF are $A(\alpha)$-stable. Nørsett [20] has derived a theoretical criterion for $A(\alpha)$-stability and using this he has computed the maximum α. There are small errors in his calculations for p = 3, 4 and 6, one of which is carried over by Lambert [15, p. 242]. The correct values (based on Nørsett's criterion) are given below.

p	α
3	$86^{\circ}\ 2'$
4	$73^{\circ}\ 21'$
5	$51^{\circ}\ 50'$
6	$17^{\circ}\ 50'$

It is tempting from fig. 41 to guess that the 7-step BDF is not $A(\alpha)$-stable. This is verified by the close-up picture given in fig. 42 which shows that this formulae is not even 0-stable. But it is absolutely stable 'outside' the boundary locus curve.

It might be mentioned here that it has been asserted since 1953 that the BDF are not 0-stable for $p \geq 7$, but the first proof was published in 1972 by Cryer.

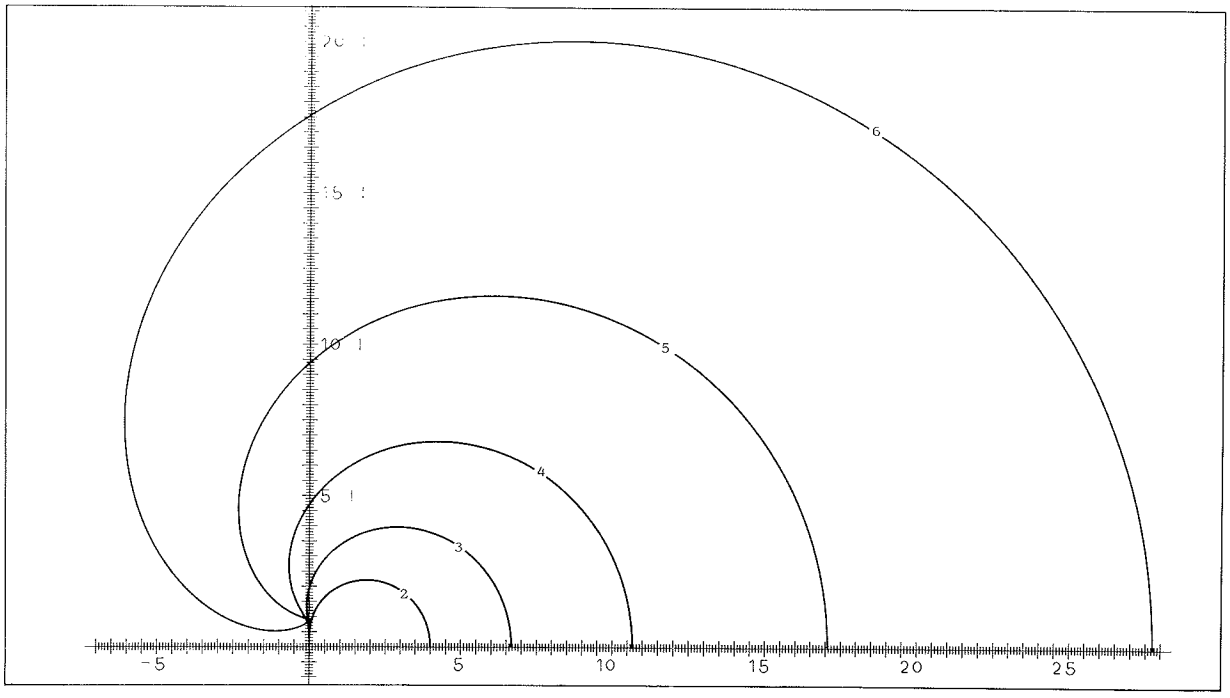

Fig. 41. BDF, p = 2, 3, 4, 5, 6.

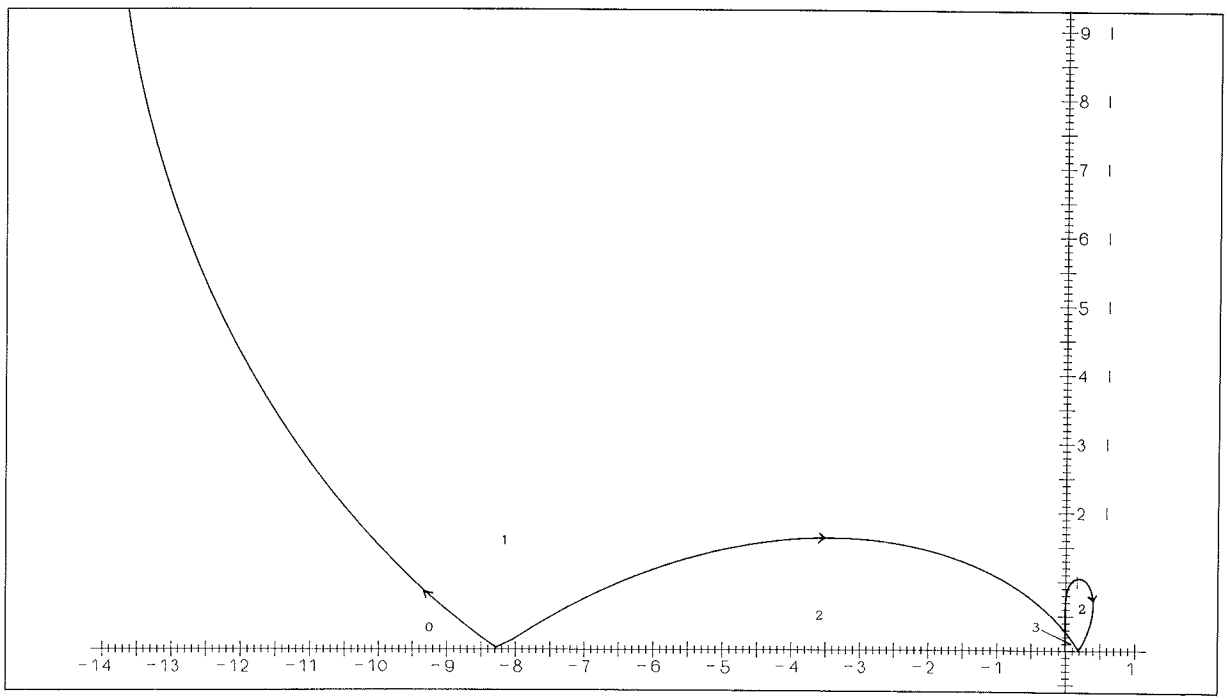

Fig. 42. BDF, p = 7.

Boundary locus curves for backward differentiation formulae.

12. Counter-Examples due to Cryer and Jeltsch

With the hierarchy of stability concepts : $\{A_0\text{-}, A(0)\text{-}, A(\alpha)\text{-}, \text{stiff}\}$ the following questions have in the past been asked : Is an A_0-stable method also A(0)-stable ? and : Is an $A(\alpha)$-stable method always stiffly stable : Both these questions have been answered in the negative by the following examples of linear multistep formulae given by Cryer [5] and Jeltsch [13].

Fig. 43, 44 and 45 show three different ways for an A_0-stable method to avoid being A(0)-stable :

Fig. 43 : $$y_{n+2} - y_{n+1} = \frac{1}{4} \cdot h \cdot (f_{n+2} + 2f_{n+1} + f_n).$$ (Cryer)

Fig. 44 : $$y_{n+3} - y_{n+2} + y_{n+1} - y_n = h \cdot (2f_{n+3} + f_{n+1} - f_n).$$ (Jeltsch)

Fig. 45 : $$y_{n+3} - \frac{4}{3}y_{n+2} + y_{n+1} - \frac{2}{3}y_n = \frac{2}{3} \cdot h \cdot (f_{n+3} + f_{n+1}).$$ (Jeltsch)

The last example, due to Jeltsch, shows an $A(\alpha)$-stable method ($\alpha = \arctan 4\sqrt{2} \doteq 79^\circ 59'$) which is not stiffly stable :

Fig. 46 : $$y_{n+3} - \frac{1}{2}y_{n+2} - \frac{1}{2}y_n = h \cdot (\frac{3}{2}f_{n+3} - f_{n+2} + \frac{3}{2}f_{n+1}).$$

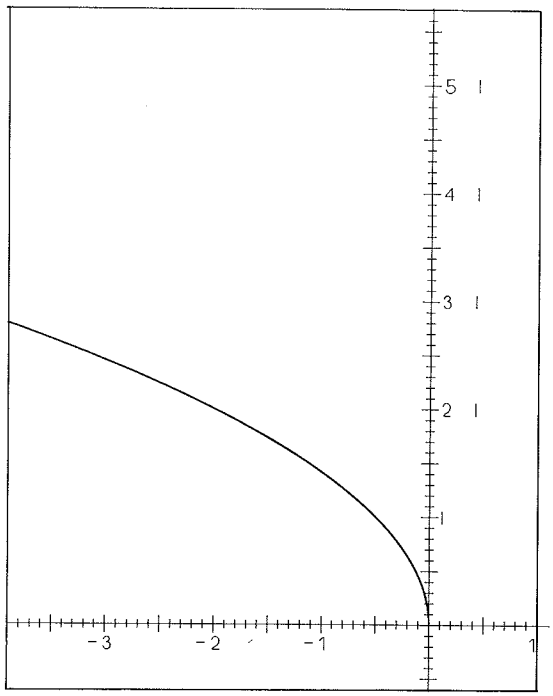

Fig. 43.

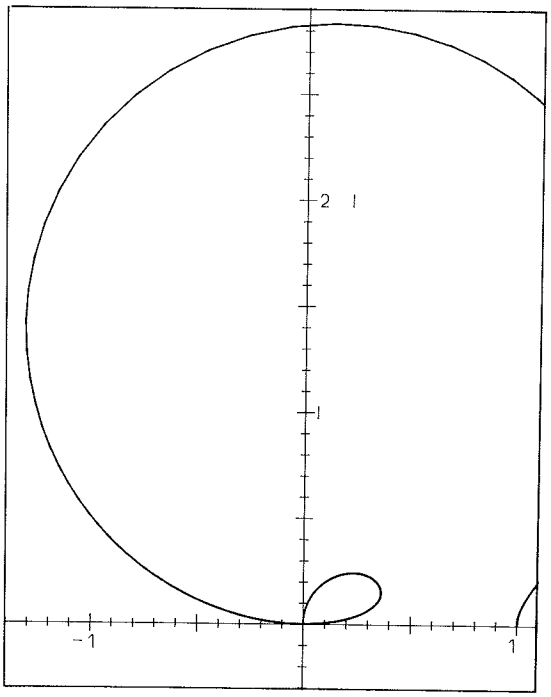

Fig. 44.

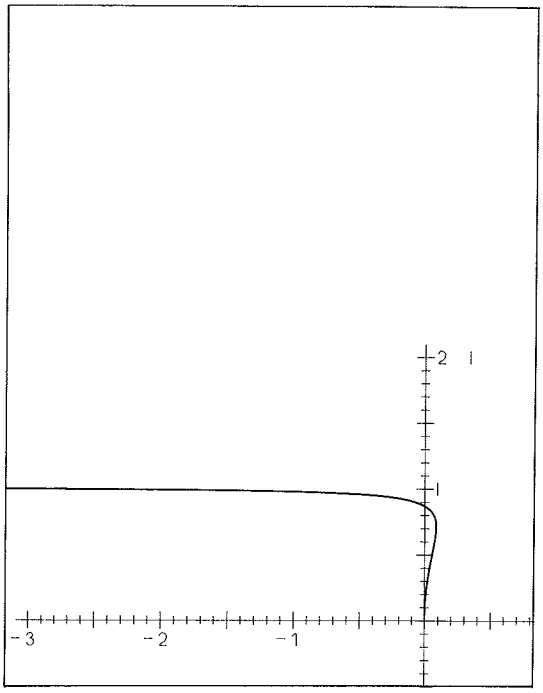

Fig. 45.

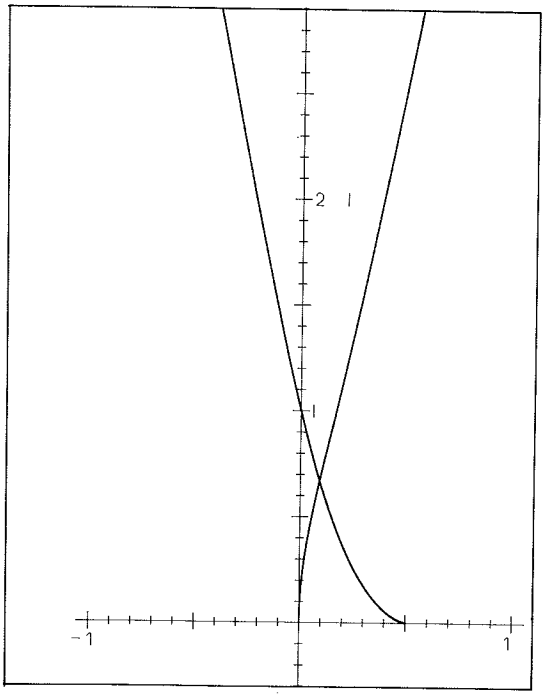

Fig. 46.

Boundary locus curves.

13. Other Contour Lines

What we have done so far can be viewed upon as drawing contours corresponding to height 1 for the surfaces that describe the magnitudes of the roots of the stability polynomial. How about other heights ? The answer to this question can be used to give more information on those surfaces and thereby give an idea on the sensitivity of a method to small perturbations. We believe that this information can be valuable when trying to produce new methods according to desired specifications by combining well-known formulae.

A more immediate use of contours corresponding to heights less than 1 is for the study of exponential stability properties of methods [29, p. 183]. Contours on both sides of 1 can also be very useful for relative stability considerations where we compare the roots of the stability polynomial with exp (Re($\bar{h}$)) [15, p. 79].

A rather interesting picture is seen for the 4 stage, 4th order Runge-Kutta methods where contours are drawn for heights 1.4, 1.2, 1.0 and 0.8 in fig. 47 and for heights 1.0, 0.8, 0.6, 0.4 in fig. 48. The figures indicate the presence of two saddlepoints and three minima inside the full region of absolute stability. It is interesting to compare this with the stability region of Scraton's method (fig. 32) and with the contours for the second order Runge-Kutta methods [29, p. 183].

We have also selected the fourth order Adams-Bashforth method for further inspection because of its simple, yet interesting boundary locus curve. In each of figs. 49-52 we show the boundary locus curve together with one contour ($1-\delta$) less than 1 and two ($1+\delta$, $1+2\delta$) larger than 1, where δ = 0.05, 0.1, 0.2 and 0.4, respectively. In this way one of the 'outside' contours is repeated from one figure to the next, which may help in the identification. With reference to exponential stability we read from the figures that the largest root in the stability region is always larger than 0.8.

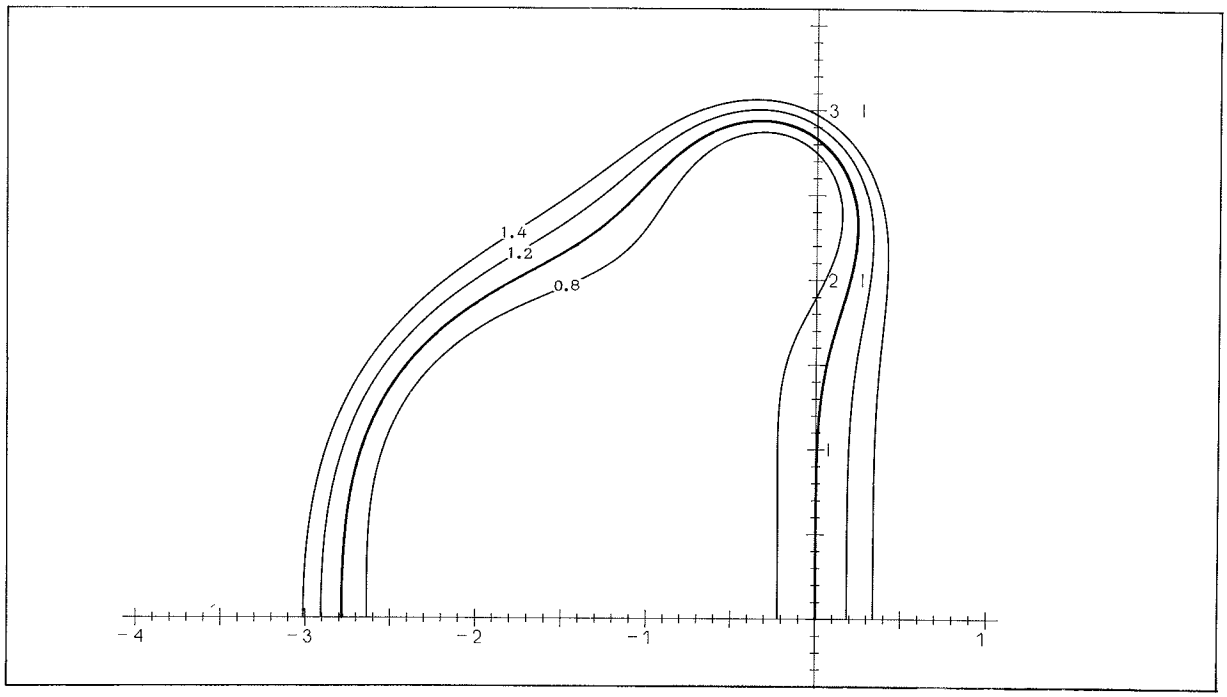

Fig. 47. RK 4, Contours 1.4, 1.2, 1.0, 0.8.

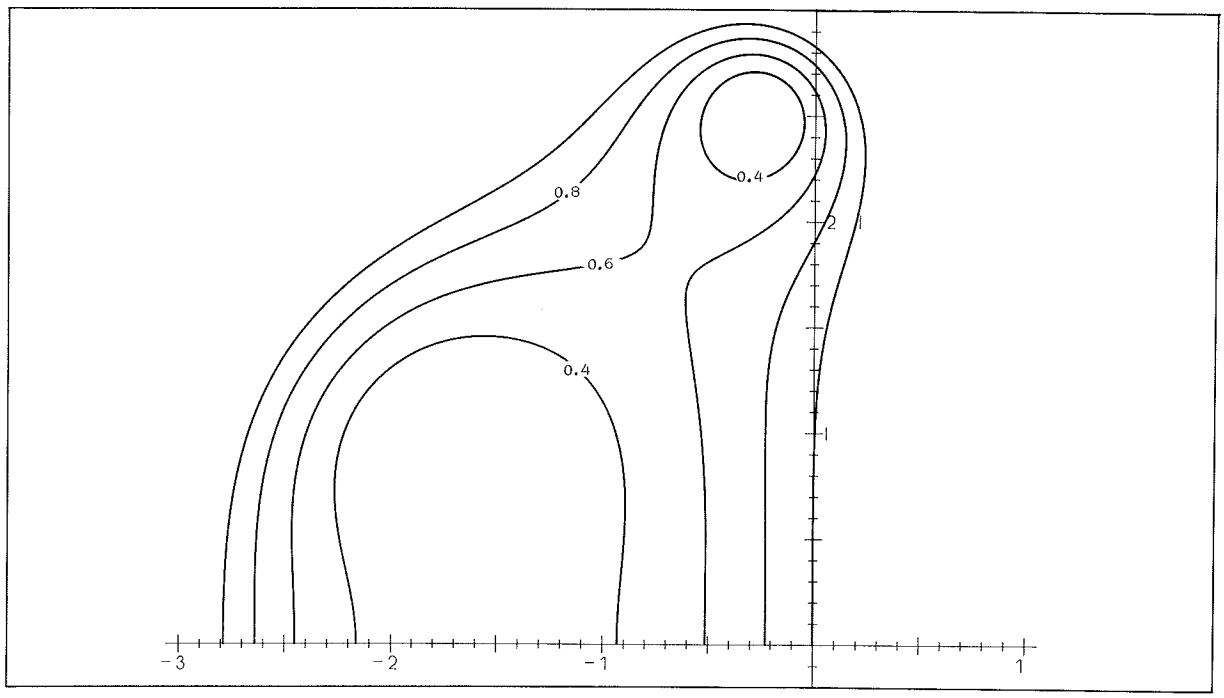

Fig. 48. RK 4, Contours 1.0, 0.8, 0.6, 0.4.

Contours for fourth order Runge-Kutta methods.

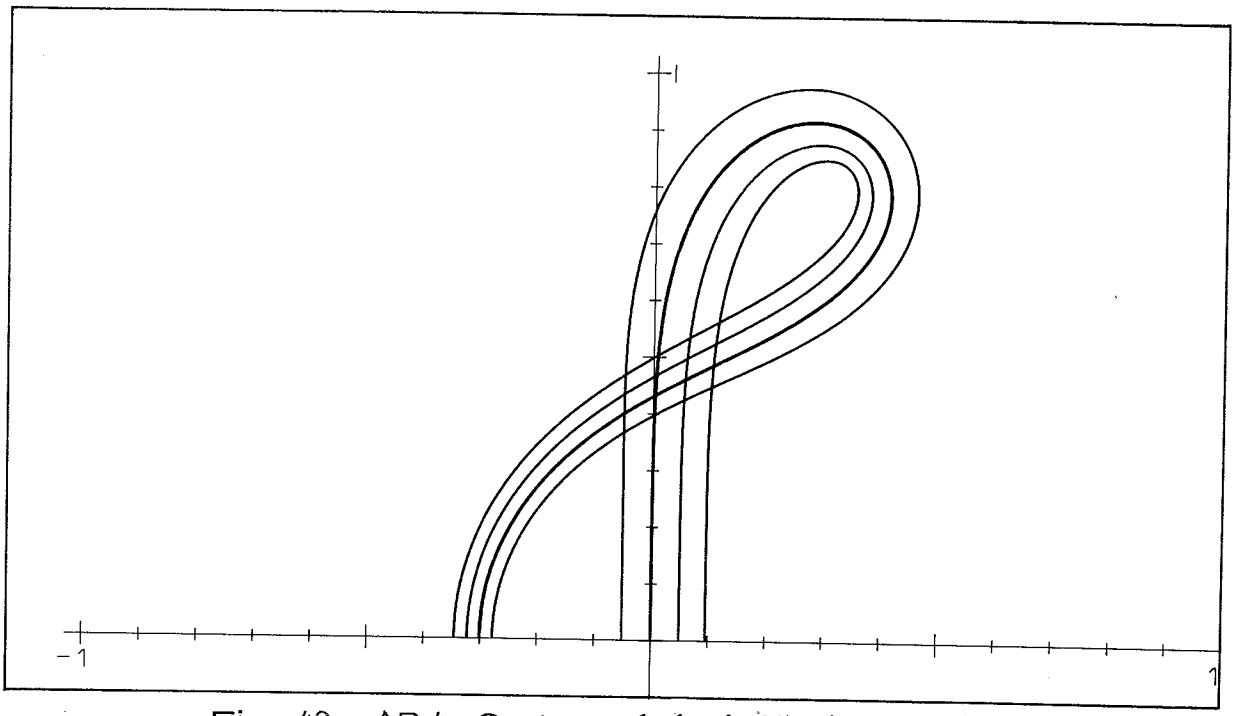

Fig. 49. AB 4, Contours 1.1, 1.05, 1.0, 0.95.

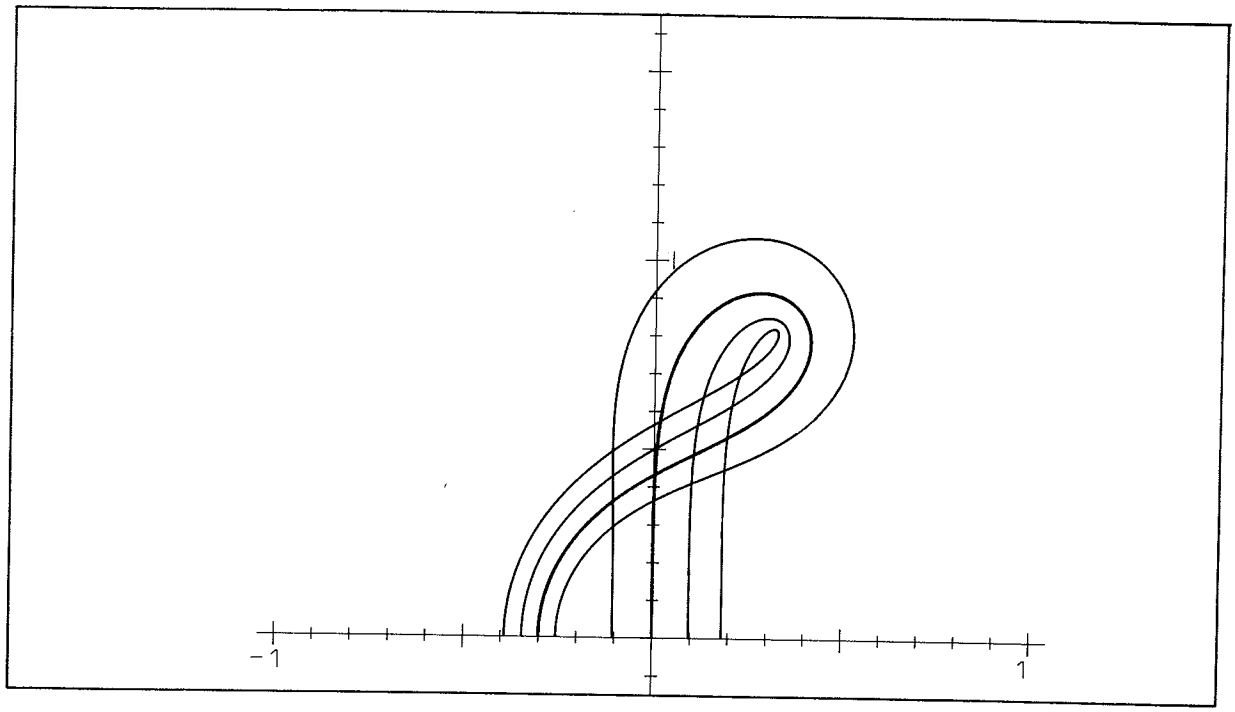

Fig. 50. AB 4, Contours 1.2, 1.1, 1.0, 0.9.

Contours for the fourth order Adams-Bashforth method.

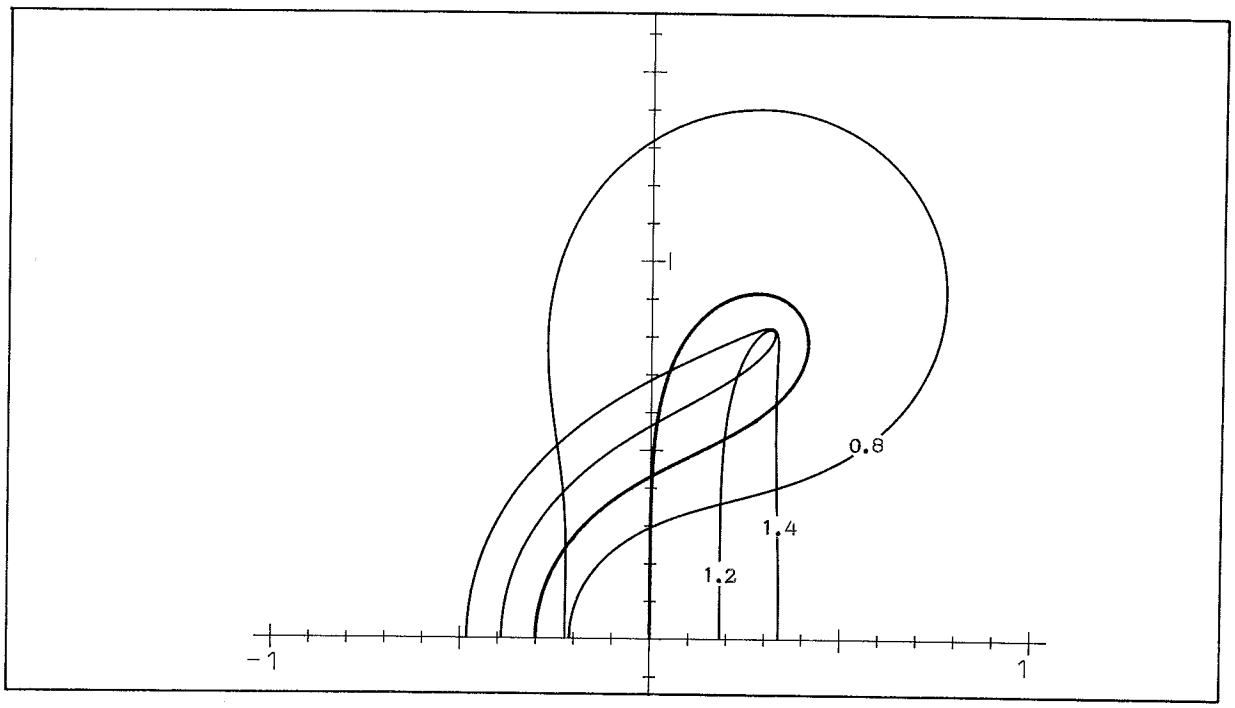

Fig. 51. AB 4, Contours 1.4, 1.2, 1.0, 0.8.

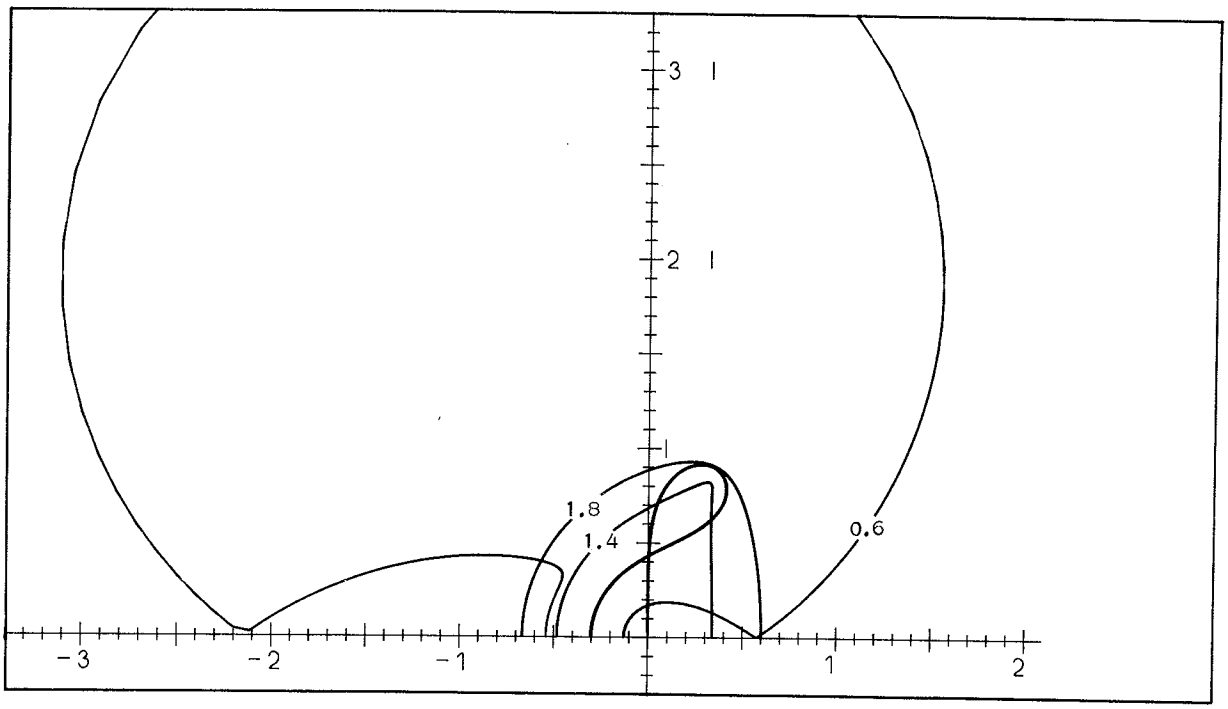

Fig. 52. AB 4, Contours 1.8, 1.4, 1.0, 0.6.

Contours for the fourth order Adams-Bashforth method.

Acknowledgements

The authors would like to express their appreciation of the work of Johan Evald Mogensen who constituted 1/3 of the SØM group during the early stages of the development. Thanks are also due to Per Grove Thomsen for illuminating discussions and valuable suggestions.

References

1. G. Birkhoff and R.S. Varga : Discretization Errors for Well-set Cauchy Problems, I, J. Math. and Phys. 44 (1965) 1-23.

2. R.R. Brown, J.D. Riley and M.M. Bennett : Stability Properties of Adams-Moulton Type Methods, Math. Comp. 19 (1965) 90-96.

3. J.C. Butcher : Implicit Runge-Kutta Processes, Math. Comp. 18 (1964) 50-64.

4. J.C. Butcher : Integration Processes Based on Radau Quadrature Formulas, Math. Comp. 18 (1964) 233-244.

5. C.W. Cryer : A New Class of Highly-stable Methods : A_0-stable Methods, BIT 13 (1973) 153-159.

6. G. Dahlquist : Fehlerabschätzungen bei Differenzenmethoden zur numerischen Integration gewöhnlicher Differentialgleichungen, ZAMM 31 (1951) 239-240.

7. G. Dahlquist : Convergence and Stability in the Numerical Integration of Ordinary Differential Equations, Math. Scand. 4 (1956) 33-53.

8. G. Dahlquist : A Special Stability Problem for Linear Multistep Methods, BIT 3 (1963) 27-43.

9. G. Dahlquist : The Theory of Linear Multistep Methods and Related Mathematical Topics, Informal Lecture Notes, Stockholm, Royal Institute of Technology, 1976.

10. B.L. Ehle : A-stable Methods and Padé Approximations to the Exponential, SIAM J. Math. Anal. 4 (1973) 671-680.

11. C.W. Gear : The Automatic Integration of Stiff Ordinary Differential Equations, Information Processing 68, ed. A.J.H. Morrell, North-Holland Publishing Co. (1969) 187-193.

12. G. Hall : Stability Analysis of Predictor-Corrector Algorithms of Adams Type, SIAM J.N.A. 11 (1974) 494-505.

13. R. Jeltsch : Stiff Stability and its Relation to A_0- and A(0)-stability. SIAM J.N.A. 13 (1976) 8-17.

14. R. Jeltsch : Stability on the Imaginary Axis and A-stability of Linear Multistep Methods, BIT 18 (1978) 170-174.

15. J.D. Lambert : Computational Methods in Ordinary Differential Equations, John Wiley, 1973.

16. J.D. Lawson : An Order Five Runge-Kutta Process With Extended Region of Stability, SIAM J.N.A. 3 (1966) 593-597.

17. J.J.H. Miller : On the Location of Zeros of Certain Classes of Polynomials with Applications to Numerical Analysis, J. IMA 8 (1971) 397-406.

18. W.E. Milne : Numerical Solution of Differential Equations, John Wiley, 1953.

19. E.J. Nyström: Über die numerische Integration von Differentialgleichungen, Acta Soc. Sci. Fenn. 50, No. 13 (1925) 1-55.

20. S.P. Nørsett : A Criterion for A(α)-stability of Linear Multistep Methods, BIT 9 (1969) 259-263.

21. N. Obrechkoff : Neue Quadraturformeln, Abh. Preuss. Akad. Wiss. Math. Nat. Kl. 4 (1940).

22. H. Rutishauser : Über die Instabilität von Methoden zur Integration gewöhnlicher Differentialgleichungen, ZAMP 3 (1952) 65-74.

23. J. Sand : Stabilitet ved Løsning af Ikke-lineære Sædvanlige Differentialligninger, Aarhus Universitet, Matematisk Institut, Master's Thesis, 1978.

24. J. Sand: Description of the SØM System, Aarhus Universitet, Department of Computer Science, DAIMI MD-35, 1978.

25. R.E. Scraton : Estimation of the Truncation Error in Runge-Kutta and Allied Processes, Comp. J. 7 (1964) 246-248.

26. L.F. Shampine : Local Extrapolation in the Solution of Ordinary Differential Equations, Math. Comp. 27 (1973) 91-97.

27. L.F. Shampine and M.K. Gordon : Computer Solution of Ordinary Differential Equations, W.H. Freeman, 1975.

28. H.J. Stetter : Stabilizing Predictors for Weakly Unstable Correctors, Math. Comp. 19 (1965) 84-89.

29. H.J. Stetter : Analysis of Discretization Methods for Ordinary Differential Equations, Springer Verlag, 1973.

30. R.S. Varga : On Higher Order Stable Implicit Methods for Solving Parabolic Partial Differential Equations, J.Math. and Phys. 40 (1961) 220-231.

31. G. Wanner, E. Hairer and S.P. Nørsett : Order Stars and Stability Theorems, BIT 18 (1978) 475-489.

32. O. Widlund : A Note on Unconditionally Stable Linear Multistep Methods, BIT 7 (1967) 65-70.

33. A. Wolfbrandt : A Study of Rosenbrock Processes with Respect to Order Conditions and Stiff Stability, The University of Göteborg, Department of Computer Science, Report 77.01.

Appendix

Coefficients for some linear multistep formulae

The Adams-Bashforth (AB), Adams-Moulton (AM), Nyström (NY), and generalized Milne-Simpson (GMS) formulae are all special cases of a class which can be written

$$y_{n+k} - y_{n+k-s} = h \cdot \sum_{j=0}^{q} \gamma_j \nabla^j f_{n+q}$$

$$= h \cdot \sum_{j=0}^{q} \beta_j f_{n+j}$$

where $q = k - t$ and

$$s = \begin{cases} 1 & \text{for AB, AM} \\ 2 & \text{for NY, GMS} \end{cases}, \qquad t = \begin{cases} 0 & \text{for AM, GMS} \\ 1 & \text{for AB, NY} \end{cases}.$$

The coefficients β_j depend on s, t and k, and γ_j depend on s and t, but we have preferred to stay with the ordinary notation and avoid too many indices.

The following table gives the rational values of β_j, $j = 0(1)\,q$, $q = 1(1)11$ for the four formulae. The order of the formulae is $q+1$ (except for GMS, $q=2$, which is of order 4) such that we have coefficients for orders 2(1)12.

The values of γ_j, $j = 1(1)11$ and the error constants C_{p+1}, $p = 1(1)11$ can be found in the table since

$$C_{p+1} = \gamma_p = (-1)^p \cdot \beta_0 \qquad \text{(for } q = p\text{)}.$$

Note the implicit normalization, $\alpha_k = 1$, and that $\gamma_0 = 1$ for AB and AM and $\gamma_0 = 2$ for NY and GMS.

The table also contains the values of α_j, $j = 0(1)q$, $q = 1(1)11$, for the implicit backward differentiation formulae (BDF):

$$\sum_{j=0}^{q} \alpha_j \, y_{n+j} = \sum_{j=1}^{q} \frac{1}{j} \nabla^j y_{n+q} = h f_{n+q} \; .$$

The order of this formula is q such that we have coefficients for orders 1(1)11. Note the implicit normalization, $\beta_q = 1$, which is different from above. It is easy, however, to transform back to the standard normalization when using the table.

The error constants of the BDF (with $\alpha_q = 1$) are easily obtained from the coefficients since

$$C_{p+1} = \frac{-1}{\alpha_q \cdot (p+1)} \qquad \text{(for } q = p\text{)} \; .$$

q	AB	AM	NY	GMS	BDF
1	$2^*\beta_j$	$2^*\beta_j$	$1^*\beta_j$	$1^*\beta_j$	$1^*\alpha_j$
	-1	1	0	2	-1
	3	1	2	0	1
2	$12^*\beta_j$	$12^*\beta_j$	$3^*\beta_j$	$3^*\beta_j$	$2^*\alpha_j$
	5	-1	1	1	1
	-16	8	-2	4	-4
	23	5	7	1	3
3	$24^*\beta_j$	$24^*\beta_j$	$3^*\beta_j$	$3^*\beta_j$	$6^*\alpha_j$
	-9	1	-1	0	-2
	37	-5	4	1	9
	-59	19	-5	4	-18
	55	9	8	1	11
4	$720^*\beta_j$	$720^*\beta_j$	$90^*\beta_j$	$90^*\beta_j$	$12^*\alpha_j$
	251	-19	29	-1	3
	-1274	106	-146	4	-16
	2616	-264	294	24	36
	-2774	646	-266	124	-48
	1901	251	269	29	25
5	$1440^*\beta_j$	$1440^*\beta_j$	$90^*\beta_j$	$90^*\beta_j$	$60^*\alpha_j$
	-475	27	-28	1	-12
	2877	-173	169	-6	75
	-7298	482	-426	14	-200
	9982	-798	574	14	300
	-7923	1427	-406	129	-300
	4277	475	297	28	137
6	$60480^*\beta_j$	$60480^*\beta_j$	$3780^*\beta_j$	$3780^*\beta_j$	$60^*\alpha_j$
	19087	-863	1139	-37	10
	-134472	6312	-8010	264	-72
	407139	-20211	24183	-807	225
	-688256	37504	-40672	1328	-400
	705549	-46461	41193	33	450
	-447288	65112	-23886	5640	-360
	198721	19087	13613	1139	147
7	$120960^*\beta_j$	$120960^*\beta_j$	$3780^*\beta_j$	$3780^*\beta_j$	$420^*\alpha_j$
	-36799	1375	-1107	32	-60
	295767	-11351	8888	-261	490
	-1041723	41499	-31257	936	-1764
	2102243	-88547	62928	-1927	3675
	-2664477	123133	-79417	2448	-4900
	2183877	-121797	64440	-639	4410
	-1152169	139849	-31635	5864	-2940
	434241	36799	14720	1107	1089

q	AB	AM	NY	GMS	BDF
8	$3628800*\beta_j$	$3628800*\beta_j$	$113400*\beta_j$	$113400*\beta_j$	$840*\alpha_j$
	1070017	-33953	32377	-833	105
	-9664106	312874	-292226	7624	-960
	38833486	-1291214	1173196	-31154	3920
	-91172642	3146338	-2750822	74728	-9408
	137968480	-5033120	4154230	-116120	14700
	-139855262	5595358	-4195622	120088	-15680
	95476786	-4604594	2839756	-42494	11760
	-43125206	4467094	-1208066	182584	-6720
	14097247	1070017	473977	32377	2283
9	$7257600*\beta_j$	$7257600*\beta_j$	$113400*\beta_j$	$113400*\beta_j$	$2520*\alpha_j$
	-2082753	57281	-31648	729	-280
	20884811	-583435	317209	-7394	2835
	-94307320	2687864	-1431554	33868	-12960
	252618224	-7394032	3831628	-92390	35280
	-444772162	13510082	-6738470	166582	-63504
	538363838	-17283646	8141878	-207974	79380
	-454661776	16002320	-6854054	181324	-70560
	265932680	-11271304	3979084	-68738	45360
	-104995189	9449717	-1492898	189145	-22680
	30277247	2082753	505625	31648	7129
10	$479001600*\beta_j$	$479001600*\beta_j$	$7484400*\beta_j$	$7484400*\beta_j$	$2520*\alpha_j$
	134211265	-3250433	2046263	-42505	252
	-1479574348	36284876	-22551398	473164	-2800
	7417904451	-184776195	113017629	-2400729	14175
	-22329634920	567450984	-340034124	7335888	-43200
	44857168434	-1170597042	682602678	-15023790	88200
	-63176201472	1710774528	-960397296	21705672	-127008
	63716378958	-1823311566	967079178	-22652334	132300
	-46113029016	1446205080	-697919124	17067984	-100800
	23591063805	-890175549	354701379	-6449433	56700
	-8271795124	656185652	-118993898	12908620	-25200
	2132509567	134211265	35417513	2046263	7381
11	$958003200*\beta_j$	$958003200*\beta_j$	$7484400*\beta_j$	$7484400*\beta_j$	$27720*\alpha_j$
	-262747265	5675265	-2008375	37888	-2520
	3158642445	-68928781	24138388	-459273	30492
	-17410248271	384709327	-133012023	2557004	-169400
	58189107627	-1305971115	444399504	-8652249	571725
	-131365867290	3007739418	-1002797874	19838928	-1306800
	211103573298	-4963166514	1610471928	-32528046	2134440
	-247741639374	6043521486	-1888266546	39209928	-2561328
	214139355366	-5519460582	1629842928	-35155374	2286900
	-135579356757	3828828885	-1029300999	23319504	-1524600
	61633227185	-2092490673	465162004	-8533273	762300
	-19433810163	1374799219	-141086023	13325388	-304920
	4527766399	262747265	37425888	2008375	83711

Coefficients for Padé approximations to the exponential function

The Padé approximations to the exponential function may be written in the form

$$R_t^s(z) = \frac{P_{s,t}(z)}{Q_{s,t}(z)}$$

where

$$P_{s,t}(z) = \sum_{j=0}^{s} \frac{(s+t-j)!\ s!}{(s-j)!\ j!}\ z^j$$

$$= \sum_{j=0}^{s} a_j(s,t) \cdot z^j \ ,$$

and

$$Q_{s,t}(z) = P_{t,s}(-z).$$

The following table contains the values of $a_j(s,t)$, j=0(1)s, s=0(1)6, t=0(1)6.

s \ j	0	1	2	3	4	5	6
0	1						
1	1	1					
2	2	2	1				
3	6	6	3	1			
4	24	24	12	4	1		
5	120	120	60	20	5	1	
6	720	720	360	120	30	6	1

t = 0

s \ j	0	1	2	3	4	5	6
0	1						
1	2	1					
2	6	4	1				
3	24	18	6	1			
4	120	96	36	8	1		
5	720	600	240	60	10	1	
6	5040	4320	1800	480	90	12	1

t = 1

s \ j	0	1	2	3	4	5	6
0	2						
1	6	2					
2	24	12	2				
3	120	72	18	2			
4	720	480	144	24	2		
5	5040	3600	1200	240	30	2	
6	40320	30240	10800	2400	360	36	2

t = 2

s \ j	0	1	2	3	4	5	6
0	6						
1	24	6					
2	120	48	6				
3	720	360	72	6			
4	5040	2880	720	96	6		
5	40320	25200	7200	1200	120	6	
6	362880	241920	75600	14400	1800	144	6

t = 3

s \ j	0	1	2	3	4	5	6
0	24						
1	120	24					
2	720	240	24				
3	5040	2160	360	24			
4	40320	20160	4320	480	24		
5	362880	201600	50400	7200	600	24	
6	3628800	2177280	604800	100800	10800	720	24

t = 4

s \ j	0	1	2	3	4	5	6
0	120						
1	720	120					
2	5040	1440	120				
3	40320	15120	2160	120			
4	362880	161280	30240	2880	120		
5	3628800	1814400	403200	50400	3600	120	
6	39916800	21772800	5443200	806400	75600	4320	120

t = 5

s \ j	0	1	2	3	4	5	6
0	720						
1	5040	720					
2	40320	10080	720				
3	362880	120960	15120	720			
4	3628800	1451520	241920	20160	720		
5	39916800	18144000	3628800	403200	25200	720	
6	479001600	239500800	54432000	7257600	604800	30240	720

t = 6

Figures

(AB = Adams-Bashforth, AM = Adams-Moulton, ABM = Adams-Bashforth-Moulton)

Figures

(AB = Adams-Bashforth, BDF = Backward Differentiation Formula)